Received: 30 May 2022 | Revised: 16 November 2022 | Accepted: 20 November 2022

DOI: 10.1111/joa.13799

Journal of Anatomy ANATOMICAL SOCIETY WILEY

ORIGINAL ARTICLE

Truly dorsostable runners: Vertebral mobility in rhinoceroses, tapirs, and horses

Ruslan I. Belyaev[1] | Alexander N. Kuznetsov[1,2] | Natalya E. Prilepskaya[1]

[1]A.N. Severtsov Institute of Ecology and Evolution, Russian Academy of Sciences, Moscow, Russian Federation

[2]Borissiak Paleontological Institute, Russian Academy of Sciences, Moscow, Russian Federation

Correspondence
Ruslan I. Belyaev, A.N. Severtsov Institute of Ecology and Evolution, Russian Academy of Sciences, 34 Vavilova Street, Moscow 119334, Russian Federation.
Email: belyaev.ruslan@gmail.com

Funding information
Russian Science Foundation, Grant/Award Number: 22-24-00885

Abstract

The vertebral column is a hallmark of vertebrates; it is the structural basis of their body and the locomotor apparatus in particular. Locomotion of any vertebrate animal in its typical habitat is directly associated with functional adaptations of its vertebrae. This study is the first large-scale analysis of mobility throughout the presacral region of the vertebral column covering a majority of extant odd-toed ungulates from 6 genera and 15 species. In this study, we used a previously developed osteometry-based method to calculate available range of motion. We quantified all three directions of intervertebral mobility: sagittal bending (SB), lateral bending (LB), and axial rotation (AR). The cervical region in perissodactyls was found to be the most mobile region of the presacral vertebral column in LB and SB. Rhinoceroses and tapirs are characterized by the least mobile necks in SB among odd-toed and even-toed ungulates. Equidae are characterized by very mobile necks, especially in LB. The first intrathoracic joint (T1–T2) in Equidae and Tapiridae is characterized by significantly increased mobility in the sagittal plane compared to the typical thoracic joints and is only slightly less mobile than typical cervical joints. The thoracolumbar part of the vertebral column in odd-toed ungulates is very stiff. Perissodactyls are characterized by frequent fusions of vertebrae with each other with complete loss of mobility. The posterior half of the thoracic region in perissodactyls is characterized by especially stiff intervertebral joints in the SB direction. This is probably associated with hindgut fermentation in perissodactyls: the sagittal stiffness of the posterior thoracic region of the vertebral column is able to passively support the hindgut heavily loaded with roughage. Horses are known as a prime example of a dorsostable galloper among mammals. However, based on SB in the lumbosacral part of the backbone, equids appear to be the least dorsostable among extant perissodactyls; the cumulative SB in equids and tapirs is as low as in the largest representatives of artiodactyls, while in Rhinocerotidae it is even lower representing the minimum across all odd-toed and even-toed ungulates. Morphological features of small Paleogene ancestors of rhinoceroses and equids indicate that dorsostability is a derived feature of perissodactyls and evolved convergently in the three extant families.

KEYWORDS
Equidae, gallop, Perissodactyla, range of motion, Rhinocerotidae, Tapiridae, vertebral biomechanics

1 | INTRODUCTION

The vertebral column is the biomechanical basis of the entire body of vertebrates. The adaptive specificity of the backbone, associated with the proportions of the different parts of the vertebral column and regionalization of mobility in the intervertebral joints, is directly related to the specifics of locomotor mode, interaction with the habitat and feeding habits (Zarnik, 1926). In recent years, the topics of backbone evolution, regionalization, and mobility have begun to gain increasing attention (Gunji & Endo, 2016; Jones et al., 2020), and the first comparative studies of intervertebral mobility in a wide range of different species have appeared (Belyaev et al., 2021b; Werneburg et al., 2015).

This study is a continuation of a series of studies on vertebral column mobility in mammals which began with artiodactyls (Belyaev, 2018; Belyaev et al. 2021b, 2022). Here, we examine the mobility of the presacral vertebral column in perissodactyls. Perissodactyla is an ancient and formerly widely diverse order of mammals (Meredith et al., 2011; Simpson, 1945; Steiner & Ryder, 2011). In contrast to the artiodactyls, the main evolutionary radiation (diversification) among odd-toed ungulates occurred as early as the Early Eocene (Prothero & Schoch, 2002). Extant perissodactyls include medium-sized and large herbivores belonging to three families: Tapiridae, Rhinocerotidae, and Equidae.

The Tapiridae is represented by medium to large-sized animals (up to 400 kg for the Malayan tapir), which mainly inhabit forests (Wilson & Mittermeier, 2011). The morphology of the tapirid postcranial skeleton is archaic for the order and very similar to that of the small Paleogene perissodactyls (Cope, 1873; Holbrook, 2001; Radinsky, 1965). The tapir body plan is characterized by a dorsally arched lumbosacral part of the backbone.

Representatives of the Rhinocerotidae are among the largest terrestrial mammals today. Moreover, the white and greater one-horned rhinoceroses are the largest extant animals that have retained the ability to use a specific fast-running mammalian gait, the gallop (Alexander & Pond, 1992). The largest mammals belonging to other orders no longer use a gallop on land. The terrestrial running gait of elephants is exclusively the fast walk with no unsupported phases (Gambaryan, 1974; Gambaryan & Ruhkyan, 1974; Hutchinson et al., 2003). The terrestrial running gait of the common hippo is the trot, although it still employs a gallop to run underwater (Coughlin & Fish, 2009).

Extant representatives of the Equidae are well-known for their excellent running speed and stamina. Horses are a prime example of the dorsostable gallop, in contrast to the dorsomobile gallop of various carnivores (Gambaryan, 1974; Hildebrand, 1959).

As was shown by Alexander et al. (1985), the storage and recoil of elastic energy in the aponeurosis of the *m. longissimus thoracis et lumborum* allows mammals to reduce metabolic costs of running by means of gallop and makes the gallop the most energy-efficient gait at high speeds. The study of vertebral biomechanics in perissodactyls, and of their vertebral range of motion (ROM) in particular, has a long history, but all previous studies were devoted to only one species, the domestic horse (*Equus ferus caballus*). Two different approaches have been used to study ROM in horses. One is the measurement of used ROM (uROM) or 'movement' in living animals (in vivo studies). The other is the measurement of available ROM (aROM) or 'mobility' on syndesmological specimens of vertebral columns (so-called in vitro studies). In most detailed studies, all three directions of intervertebral movement or mobility were analyzed: sagittal bending (SB), lateral bending (LB), and axial rotation (AR).

The first study of vertebral column amplitudes of mobility in the domestic horse examined SB aROM in the lumbosacral joint (Pylypchuk, 1975). The amplitude of mobility was measured on X-ray photographs. In a later study, Townsend with co-authors measured all three directions of mobility (SB, LB, and AR) in the whole thoracolumbar part of the backbone (Townsend et al., 1983), and in the cervical region (Clayton & Townsend, 1989a, 1989b). The amplitudes of mobility (aROM values) were measured on photographs. These studies did not adhere to approved techniques of human medical biomechanics employing a special spine tester which ensures loading of each intervertebral joint with a standardized torque value (see White & Panjabi, 1990). The whole lumbar (Pylypchuk, 1975) or cervical (Clayton & Townsend, 1989a, 1989b) region or even the whole thoracolumbosacral backbone (Townsend et al., 1983) were bent without segmentation into functional spinal units (FSU)—pairs or triples of vertebrae used in such experiments today.

Subsequent studies of amplitudes of vertebral column in vivo movements (uROM) in the domestic horse were performed by kinematic analysis of markers fixed on the skin or implanted into the dorsal spinous processes of the vertebrae. Numerous studies have provided data on the SB, LB, and AR movements of the vertebral column while animals were walking, trotting, and cantering on a treadmill (Audigié et al., 1999; Faber et al., 2000, 2001a, 2001b, 2002; Haussler et al., 1999, 2001; Pourcelot et al., 1998; Wennerstrand et al., 2009). Most of these papers focused on the lumbar region of the vertebral column. Markers were fixed either on certain vertebrae in the thoracic, lumbar, and sacral regions (Audigié et al., 1999; Faber et al., 2000, 2001a, 2001b, 2002; Pourcelot et al., 1998; Wennerstrand et al., 2009) or on several consecutive vertebrae in the same region of the vertebral column (Haussler et al., 1999, 2001). In the first case, regional vertebral kinematics, and in the second case, segmental vertebral kinematics between adjacent vertebrae were assessed.

Representatives of the three extant families of perissodactyls are quite different from each other and have a specific and easily distinguishable appearance. The dorsally arched and relatively short-legged tapirs are primarily adapted to the forest habitat, whereas huge rhinoceroses represent the largest habitually galloping animals, and relatively long-legged and long-necked equids are well-adapted to foraging and dorsostable galloping in the open landscape. The substantial differences in body plan must certainly be reflected in the specificity of the mobility of backbone. However, the mobility of the vertebral column in Tapiridae, Rhinocerotidae, and Equidae, with the exception of the domestic horse, remains poorly explored. The purpose of this study is to obtain the first quantitative overview

of the three directions of mobility throughout the presacral region of the vertebral column in extant odd-toed ungulates. Among other questions in this study, we want to assess: the extent to which the long neck of equids is a more mobile manipulator than the short neck of tapirs and rhinoceroses; the functional role of elongated (compared to artiodactyls, carnivores, etc.) thoracic region of perissodactyls; and the degree of SB mobility in the lumbosacral part of the backbone of the largest galloping mammals. The mobility of the cervical, thoracic, and lumbar regions as well as divisions with different zygapophysial facet articulations in perissodactyls are analyzed in comparison with previously published data on artiodactyls.

2 | MATERIALS

Only dry osteological material stored in collections was used. The studied material belongs to the following collections: Naturhistorisches Museum Wien (NMW), Austria; Rostov-on-Don Zoo (RZ), Rostov-on-Don; Zoological Institute of the Russian Academy of Sciences (ZIN), Saint Petersburg; Zoological Museum of the Lomonosov Moscow State University (ZMMU), Moscow. Overall, this study covers representatives of all three extant perissodactyl families: three of four species of tapirs, all five species of rhinoceroses, and all seven species of equids (following modern taxonomy: Ruiz-García et al., 2016; Vilstrup et al., 2013; Wilson & Mittermeier, 2011) (Table S1). For comparison, we used a dataset of 52 specimens of artiodactyls in which mobility in the entire presacral region of the vertebral column has been previously studied (Belyaev et al., 2021b; Table S1). We excluded juveniles because they have been shown to differ from adults in vertebral morphology (Benninger et al., 2004); any specimen with end-plates un-fused to the vertebral bodies was considered juvenile. Most of the studied perissodactyls (and previously studied artiodactyls) were animals kept in captivity. Life in captivity can lead to an increased number of pathologies (including backbone pathologies) and changes in bone morphology compared with animals living in the wild (Canington et al., 2018; O'Regan & Kitchener, 2005). Thus, the results obtained here may differ to some extent from a sample of the same species from the wild.

2.1 | Terminology for vertebral column parts

Regions—cervical, thoracic, lumbar, sacral—are traditionally defined by rib features: cervical ribs are pleurapophyses, thoracic ribs are free, lumbar ribs are absent or fused to transverse processes (Filler, 2007), and sacral ribs mediate sacroiliac fusion (Figure 1). Neck mobility refers to intracervical joints posterior to the axis—C2–C7. Thoracic region mobility refers to intrathoracic joints from T1–T2 up to the joint between the penultimate and ultimate thoracic vertebrae. Lumbar region mobility refers to intralumbar joints from L1–L2 up to the joint between the penultimate and ultimate lumbar vertebrae. Lumbosacral mobility refers to all the intralumbar plus the lumbosacral joint—L1–S1. In this study, we assigned the neck-thorax joint (C7–T1) to the cervical region and the joint located between the last thoracic vertebra and L1 as well as the lumbosacral joint to the lumbar region. So, referring to the thoracic region we will mean intrathoracic joints only.

When reasonable, we will separately treat anterior and posterior halves of the thoracic region. When the number of intrathoracic joints is even, the two halves include equal numbers of joints. With an odd number of intrathoracic joints, the anterior half is regarded as having one more joint than the posterior half.

Divisions—are distinguished by zygapophysial facet type. From anterior to posterior end of the presacral vertebral column there is a succession of radial facets (Rf), tangential facets (Tf), and radial facets with a lock (RfL) (Figure 1c–f). Transitional vertebra with Rf prezygapophyses and Tf postzygapophyses is usually T1 but sometimes T2. Transitional vertebra with Tf prezygapophyses and RfL postzygapophyses, historically termed "diaphragmatic vertebra" (Slijper, 1946), varies in position from posterior part of thoracic region to the ultimate lumbar vertebra.

3 | METHODS

We used our previously established mechanistic approach—based on vertebral osteometry—to calculate intervertebral mobility (Belyaev et al., 2021a). This approach is based on the assumption of a functional interrelation between aROM and the geometry of vertebrae and especially of articular facets (Kuznetsov & Tereschenko, 2010). Trigonometric formulae are used for aROM calculation.

In this study, we calculated the amplitudes (aROM values) for three degrees of freedom in every presacral intervertebral joint except the atlas-axis (number 1). For SB the calculated amplitude of motion is the sum of ventral flexion and dorsal extension, and for LB and AR, it is the sum of respective motions to the left and to the right. Both the mean amplitudes of motion in the intervertebral joints and the cumulative aROM values (sum of aROMs in the intervertebral joints of different regions and divisions of the vertebral column) will be analyzed.

Our model is designed to derive syndesmological aROM estimates from dry vertebrae osteometry with the help of a pair of adjustable coefficients (K_S and K_R; Figure 2). Their values were adjusted so as to match the estimate to direct in vitro aROM measurements on syndesmological preparations of vertebral columns of a few reference species of artiodactyls (sheep, pig, and cow) (Wilke et al., 1997a, 1997b, 2011). Thus, the calibrated formulae allow us to calculate syndesmological aROMs based on vertebrae osteometry. The approach comes from the idea that articular surfaces resemble segments of surfaces of rotation. Therefore, an angle of rotation in a chosen projection can be calculated (in radians) by dividing the length of an arc of rotation by the radius of this arc. The length of the arc of rotation is calculated from the difference of lengths of the arcs of two articulating surfaces, and from their maximum non-overlap constraint introduced with a coefficient K_S.

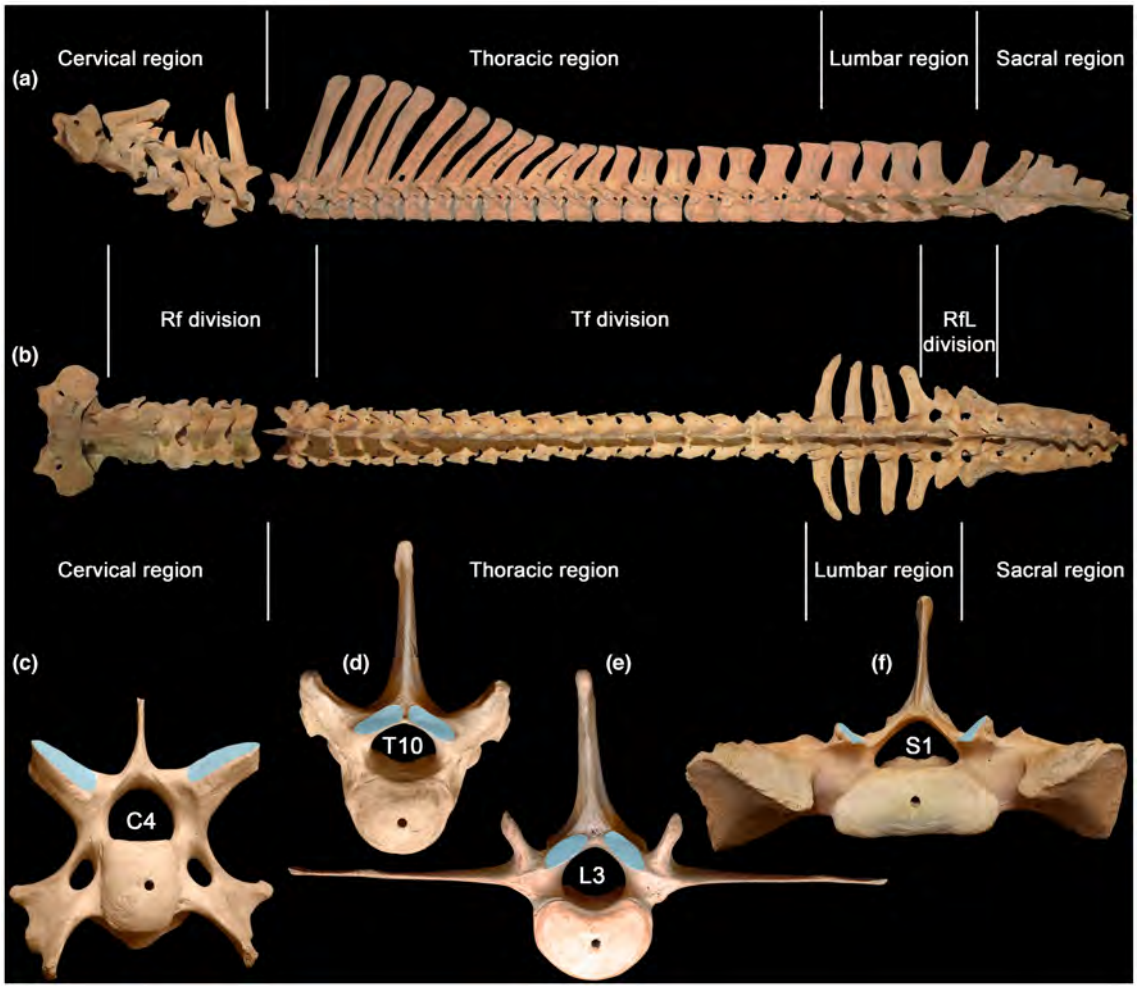

FIGURE 1 Regions (cervical, thoracic, lumbar, and sacral) and divisions (radial (Rf), tangential (Tf), and radial with a lock (RfL) facet types) of the vertebral column exemplified by *Tapirus bardii* (ZMMU S-102033). Left lateral (a) and dorsal (b) view of the entire vertebral column. (c)–(f) Anterior view of selected vertebrae showing different orientations of prezygapophysial articular facets: Rf in C4 (c), Tf in T10 (d) and L3 (e), RfL in S1 (f). Zygapophysial facets highlighted with blue color.

More specifically, K_S determines the fraction of the smaller facet which slides out of the larger one in the marginal positions of joint motions. The second coefficient K_R adjusts the radius of rotation in the joint (see Figure 2).

In the course of evaluation of the optimal formulae for calculating aROM values, it was found that separate formulae for different zygapophysial facet types (Rf, Tf, RfL) give significantly greater accuracy in aROM calculation than the formulae for the presacral vertebral column as a whole, and greater accuracy than the separate formulae for different vertebral column regions (cervical, thoracic, lumbar) (Belyaev et al., 2021a). Thus, the K_S and K_R coefficients are zygapophysial facet-specific (Rf, Tf, and RfL) and mobility-specific (SB, LB, and AR), and hence, there are $3 \times 3 = 9$ optimal specific values of each coefficient for the whole vertebral column. The correspondence of calculated aROM and in vitro aROM curves in the reference species (sheep, pig, and cow) throughout the presacral spine length was checked by calculating Pearson correlation coefficients (r). Student's t-test (paired samples) was used to show that the differences between the calculated and in vitro aROMs in the joint-by-joint values of the reference species were not significant (Belyaev et al., 2021a).

As in our previous study on even-toed ungulates (Belyaev et al., 2021b), the formulae were calibrated with in vitro data of sheep, pig, and cow (Wilke et al., 1997a, 1997b, 2011). We had no other choice because similar (in terms of completeness and reliability) in vitro data are not available for any of the odd-toed ungulates, even for the domestic horse. And the use of in vivo studies of live vertebral column movements for calibration would lead to a significant mistake: in horses, such studies are usually carried out on a treadmill, which greatly limits the animal's ability to display the full uROM in all three directions (especially LB and AR). Direct comparisons of in vivo (Faber et al., 2000, 2001a, 2001b; Haussler et al., 1999, 2001; Wennerstrand et al., 2009) and in vitro data (Pylypchuk, 1975; Townsend et al., 1983) show that SB and LB uROM amplitudes are always significantly lower than aROM. This mismatch between uROM and aROM is the result of an artifact of the treadmill experiments. Maximum uROM values can be demonstrated by an animal only during running (SB) and maneuvering (LB

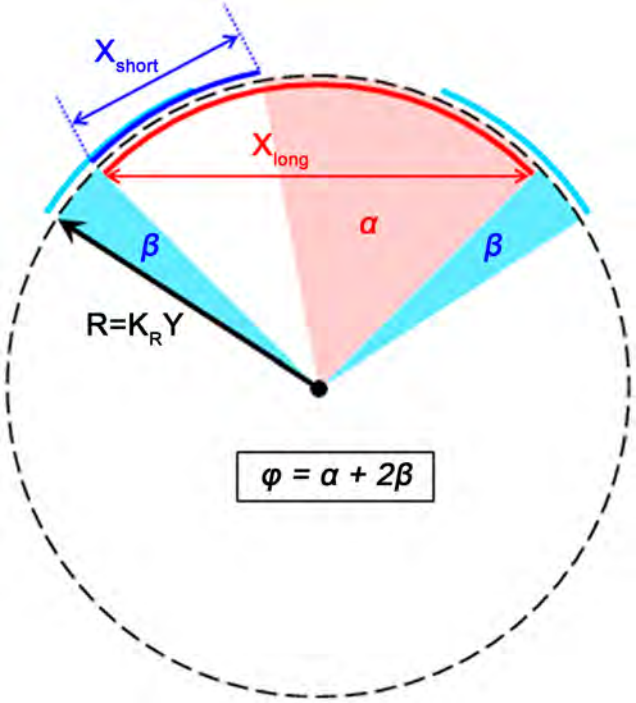

FIGURE 2 The scheme of the mechanistic model for calculation formulae of intervertebral aROM based on dimensions of vertebrae. In the plane of motion, the zygapophysial facets of the two adjacent vertebrae are treated as arcs of equal radius R (black arrow). One facet is usually smaller (blue arc) than the other (red arc), and their sizes are measured by respective chords X_{short} and X_{long}. The radius R of the facet arcs' curvature is treated as the radius of joint rotation and is derived from one or the other dimension Y of the vertebrae with the multiplication coefficient K_R, which is subject to empirical adjustment. Finally, aROM consists of two terms. The first one represents the available shift of the smaller facet in the limits of the larger one, which is equal to the angular difference α between the larger and the smaller facets (pale red sector). The second term represents the available shift of the smaller facet beyond the larger one to every side, which is equal to angular overhanging β of the smaller facet in the marginal positions (two pale blue sectors).

and AR) at the limit of its abilities, which is impossible during treadmill experiments. In laboratory conditions, only humans can voluntarily demonstrate the most complete uROM, which is necessary for comparison with aROM. Various medical studies of human vertebral biomechanics show that uROM and aROM values are mostly similar (Yamamoto et al., 1992; Panjabi et al., 1994, 2001; Wilke et al., 2017; see also our summary of these data in Belyaev et al. 2021a, 2022).

The use of the same coefficients to calculate aROM in odd-toed (this study) and even-toed (Belyaev et al., 2021b) ungulates ensures that all the intergroup/interspecific differences in aROMs subsequently identified in this study are associated with the geometry of the vertebrae, and nothing else. The formulae represented in Table 1 are exactly the same as those used by Belyaev et al. (2021b). The measurements used are shown and explained in detail by Belyaev et al. (2021a; Figure 1 and figure S2 therein) and depicted in Figure 3 herein. A workflow showing how aROM values are calculated is presented in tables S1–S4 in Belyaev et al. (2021a). The modified SB formula for the lumbosacral joint (Belyaev et al., 2022) is not suitable for perissodactyls because they lack a well-pronounced prezygapophysial postfacet fossa with stopper on the first sacral vertebra. Thus, SB aROM in the lumbosacral joints in perissodactyls is calculated with the same formula as for RfL interlumbar joints, while in artiodactyls it was calculated (Belyaev et al., 2022) with the special formula taking the postfacet stopper into account.

3.1 | Single-axis rotations versus combined motions

For a long period of time, joint rotations were measured separately in each of the three orthogonal planes. Thus, different degrees of freedom (DoFs) were studied separately, one by one, as independent deviations from some neutral position. Combined motions were previously presented mainly in the anatomical atlases intended for artists. However, over the last few years in vitro data on combined joint motions have become more frequently presented. For instance, the syndesmological aROM was presented for circumduction (combined flexion–extension and adduction–abduction) in the bat shoulder joint (Panyutina et al., 2013). Among the most methodologically advanced in vitro studies of combined aROM, are recent studies of the turkey's neck (Kambic et al., 2017) and of the echidna's forelimb (Regnault et al., 2021). Combined motions in a joint are interesting because they are often used by animals and, therefore, the interdependencies between ROMs across different DoFs may be important. However, the research of combined motions raises new methodological problems which can be illustrated by the papers just cited. First, the combined motion is performed by an experimenter via ropes (Panyutina et al., 2013) or sticks (Kambic et al., 2017; Regnault et al., 2021) attached to the subject. This may lead to articular surfaces being less closely articulated than in living animals developing muscle contraction. Therefore, the procedure is potentially confounded by disarticulation and consequent aROM overestimation. Second, an additional overestimation of translational amplitudes can come from the use of geometric primitives (e.g., the sphere) for joint structure imitation as in Regnault et al. (2021). If the center of a chosen geometric primitive is placed away from the true center of joint rotation, the distance between the two is inevitably recalculated into a translational shift which does not exist in reality. Finding positions of instantaneous centers of rotation would be a more adequate procedure than the imposing of artificial geometric primitives. Third and the most important is the choice of a coordinate system. The problem does not arise when rotations around three orthogonal axes fixed to one of the two articulated bones are treated separately. However, when a combined rotation occurs, this coordinate system loses sense. For instance, in the echidna, the axis transverse to the body was taken for the axis of pronation-supination of the humerus (Regnault et al., 2021). However, this assumption is true only while the humerus is aligned transversely. When the humerus deflects anteriorly or posteriorly, the same transversal axis becomes,

TABLE 1 Formulae for aROM calculations were used in this study

Motion type	Facet type	Formula	K_R	K_S
SB	Rf	$\varphi = [\arcsin(L_{long}/\mathbf{1.38}\,R_{vert}) - \mathbf{0.72}\arcsin(L_{short}/\mathbf{1.38}R_{vert})] \times 360/\pi$	0.69	0.14
	Tf	$\varphi = [\arcsin(L_{long}/\mathbf{2}R_{vert}) - \mathbf{0.76}\arcsin(L_{short}/\mathbf{2}R_{vert})] \times 360/\pi$	1	0.12
	RfL	$\varphi = [\arcsin(L_{long}/\mathbf{2}R_{vert}) - \mathbf{0.64}\arcsin(L_{short}/\mathbf{2}R_{vert})] \times 360/\pi$	1	0.18
LB	Rf	$\varphi = [\arcsin(L_{long}/\mathbf{2}R_{lat}) - \mathbf{0.18}\arcsin(L_{short}/\mathbf{2}R_{lat})] \times 360/\pi$	1	0.41
	Tf	$\varphi = [\arcsin(W_{long}/\mathbf{2}R_{lat}) - \mathbf{0.52}\arcsin(W_{short}/\mathbf{2}R_{lat})] \times 360/\pi$	1	0.24
	RfL	$\varphi = [\arcsin(D_{max\_long}/\mathbf{2}R_{lat}) - \mathbf{0.86}\arcsin(D_{max\_short}/\mathbf{2}R_{lat})] \times 360/\pi$	1	0.07
AR	Rf	$\varphi = [\arcsin(W_{long}/\mathbf{2}R_{vert}) - \mathbf{0.74}\arcsin(W_{short}/\mathbf{2}R_{vert})] \times 360/\pi$	1	0.13
	Tf	$\varphi = [\arcsin(W_{long}/\mathbf{2}R_{lat}) - \mathbf{0.54}\arcsin(W_{short}/\mathbf{2}R_{lat})] \times 360/\pi$	1	0.23
	RfL	$\varphi = [\arcsin(D_{max\_long}/\mathbf{2}R_{lat}) - \arcsin(D_{max\_short}/\mathbf{2}R_{lat})] \times 360/\pi$	1	0

See measurements in Figure 3 (also Figure 1 and figure S2 from Belyaev et al., 2021a). Optimized coefficient values are specified in the right columns.

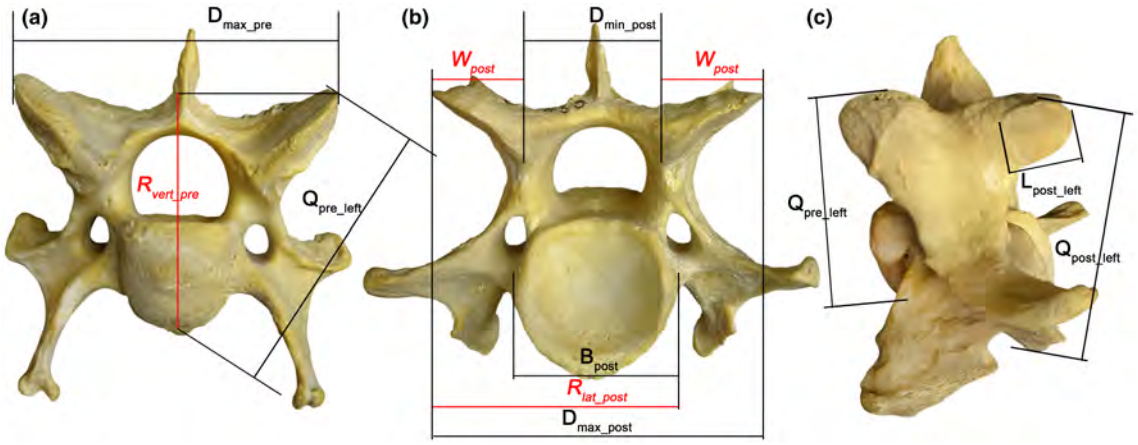

FIGURE 3 Vertebral measurements. *Tapirus terrestris* (ZMMU S-184859) vertebra C4 (Rf type) is depicted in the anterior (a), posterior (b), and left lateral (c) view. The measurements and the derived parameters (highlighted in red, italics) are shown, which are involved in aROM calculation formulae presented in Table 1.

for the humerus, the axis of depression-elevation in the parasagittal plane, instead of pronation-supination. When the humerus deflects dorsally or ventrally, the same transversal axis becomes, for the humerus, the axis of protraction-retraction in the parasagittal plane. Moreover, any combined rotation of a bone does not have a single representation in the 3D orthogonal coordinates fixed to one bone. The angles of the "free" bone relative to each of these three axes depend on the order in which the axes are referred to as the first, the second, and the third axis. To avoid this problem, a concept of "Joint Coordinate System" (JCS) was developed (Grood & Suntay, 1983). In this coordinate system, one axis of rotation is fixed to one bone in a joint, and the second axis of rotation to the other bone, so these two axes are mutually independent and generally non-orthogonal. The third axis is not fixed to any bone. It is floating to remain orthogonal to both former axes. In this approach, the only uncertainty is, which of the three anatomical axes (flexion-extension, adduction-abduction, pronation-supination) to fix to this or the other bone, and which one to retain as the floating axis. This is a choice for convention (Wu et al., 2002, 2005). The two fixed axes of JCS, if correctly positioned, correspond to the natural anatomical DoFs and thus the limits for the respective aROMs can be explained in terms of ligamentous and bony stoppers. Kambic et al. (2017) succeeded in applying the method of JCS to measure combined mobility in a turkey's neck. When studying single-axis rotations separately (as we do), the JCS coincides in fact with the classic orthogonal coordinate system fixed to one of two bones in a joint. This is a simple classic approach which we use following the available reference data from in vitro single-axis rotation experiments on the FSUs of sheep, pig, and cow (Belyaev et al., 2021a).

3.2 | Length measurements

We measured the lengths of the vertebral regions (cervical, thoracic, lumbar, sacral) and divisions (Rf, Tf, RfL) (Table S1) to study the relationship between the linear dimensions of the vertebral column and intervertebral mobility. The length was measured on the articulated vertebral columns, along the ventral sagittal line. For example, the length of the cervical region was measured from the anterior edge of C1 (atlas) to the posterior edge of C7, etc.

Based on these measurements, the following proportions were calculated: cervical region length/trunk length (the latter is thoracolumbar plus sacral length); thoracic region length/thoracolumbar length; lumbar region length/thoracolumbar length; Tf division length/thoracolumbar length; RfL division length/thoracolumbar length.

3.3 | Data analysis

Data were analyzed in IBM SPSS Statistics 23. The data analysis took into account the model limitations described in detail in previous studies (Belyaev et al. 2021a, 2021b). Data on odd-toed ungulates ($n = 29$) were analyzed together with a previously published dataset of the even-toed ungulates ($n = 52$).

Before analyzing the results, the variables were tested for normality using the Kolmogorov–Smirnov test. The K–S test results are shown in Tables 2–5. If the K–S test showed that the distribution was normal, then parametric statistics were used for further analysis. Student's *t*-test (independent samples) was used to compare the mobility in perissodactyls versus artiodactyls, as well as the mobility in perissodactyls versus artiodactyls using the same running form (sensu Gambaryan, 1974). Analysis of variance (ANOVA) was used to compare mobility in different regions and divisions of the vertebral column among various groups of perissodactyls and artiodactyls. If the K–S test showed that the sample did not have a normal distribution, then non-parametric statistics were used. The Mann–Whitney *U* test was used to compare mobility in perissodactyls versus artiodactyls using the same running form. The Kruskal–Wallis *H* test was used to compare the mobility in different regions and divisions of the vertebral column.

Alongside one-way ANOVA, three methods of Post Hoc Multiple Comparisons were used: Duncan, Scheffe, and Tukey's HSD. The Holm–Bonferroni method was used to control the family-wise error rate. Taxonomic grouping, habitat, and feeding type were used as grouping variables for ANOVA. Grouping by running forms, in perissodactyls (contrary to artiodactyls), coincides with taxonomic grouping, and therefore was not used in the current study. The feeding type was defined in the most general form and perissodactyls were divided into three groups: browsers,

TABLE 2 Numerical characteristics and length proportions of the vertebral column in perissodactyls

							Species	
Variable	*N*	Min	Max	Mean	SD	K–S test (*p*)	Min	Max
No. C+T+L vertebrae	29	28	32	30.2	0.966	0.001	Multiple	*Eq. f. przewalsii*
No. T vertebrae	28	18	20	18.5	0.694	0.000	Multiple	Multiple
No. L vertebrae	29	3	6	4.8	1.215	0.001	Multiple	Multiple
No. S vertebrae	25	4	7	5.4	0.913	0.002	Multiple	Multiple
No. Rf joints	29	6	7	6.7	0.455	0.000	Multiple	Multiple
No. Tf joints	27	14	22	17.6	2.791	0.000	*Eq. f. caballus*	*D. bicornis*
No. RfL joints	28	1	9	4.9	3.018	0.000	Multiple	*Eq. f. caballus*
Length ratio C/(T+L+S) (%)	29	21.5	51.0	37.3	0.096	0.005	*T. bardii*	*Eq. kiang*
Length ratio T/(T+L) (%)	29	71.2	88.0	77.9	0.056	0.000	*Eq. kiang*	*D. bicornis*
Length ratio L/(T+L) (%)	29	12.0	28.8	22.1	0.056	0.000	*D. bicornis*	*Eq. kiang*
Length ratio Tf/(T+L) (%)	29	61.7	96.2	79.2	0.130	0.000	*Eq. f. caballus*	*D. sumatrensis*
Length ratio RfL/(T+L) (%)	29	3.8	38.3	20.8	0.130	0.000	*D. sumatrensis*	*Eq. f. caballus*

Note: *N*, number of skeletons involved in each measurement.
Abbreviations: C, cervical; L, lumbar; S, sacral; T, thoracic.

TABLE 4 aROMs in Tf division of the vertebral column in perissodactyls

							Species	
Variable	*N*	Min (°)	Max (°)	Mean (°)	SD (°)	K–S test (*p*)	Min	Max
SB mean	21	3.67	6.17	5.02	0.57	0.200	*D. sumatrensis*	*R. sondaicus*
SB cumul	21	65.20	123.30	92.37	18.42	0.200	*E. asinus*	*R. sondaicus*
LB mean	17	8.60	12.96	11.52	1.08	0.015	*T. terrestris*	*R. sondaicus*
LB cumul	17	169.10	259.10	203.56	28.47	0.200	*E. grevyi*	*R. sondaicus*
AR mean	17	8.29	12.51	11.13	1.05	0.010	*T. terrestris*	*R. sondaicus*
AR cumul	17	163.60	250.20	196.61	27.36	0.161	*E. grevyi*	*R. sondaicus*

TABLE 3 aROMs in Rf division of the vertebral column in perissodactyls

Variable	N	Min (°)	Max (°)	Mean (°)	SD (°)	K–S test (p)	Species	
							Min	Max
SB mean	29	7.56	16.48	12.36	2.77	0.023	*T. terrestris*	*Eq. hemionus*
SB cumul	29	51.10	115.40	83.46	22.43	0.005	*D. bicornis*	*Eq. hemionus*
LB mean	25	17.46	32.70	26.88	4.15	0.200	*T. terrestris*	*Eq. f. przewalsii*
LB cumul	25	105.60	228.90	181.78	36.69	0.042	*T. terrestris*	*Eq. f. przewalsii*
AR mean	25	4.76	7.25	6.06	0.68	0.200	*C. simum*	*Eq. f. przewalsii*
AR cumul	25	28.60	50.75	41.13	6.18	0.200	*C. simum*	*Eq. f. przewalsii*

Abbreviation: cumul, cumulative.

TABLE 5 aROMs in lumbar region of the vertebral column in perissodactyls

Variable	N	Min (°)	Max (°)	Mean (°)	SD (°)	K–S test (p)	Species	
							Min	Max
SB mean	29	4.98	10.03	7.45	1.17	0.200	*D. sumatrensis*	*Eq. hemionus*
SB cumul	29	19.91	61.40	42.82	11.58	0.200	*D. sumatrensis*	*Eq. kiang*
LB mean	25	5.80	12.44	9.43	1.54	0.200	*Eq. f. przewalsii*	*T. bardii*
LB cumul	25	39.80	74.60	55.67	9.47	0.200	*D. bicornis*	*T. bardii*
AR mean	25	0.71	9.16	4.02	2.68	0.088	*Eq. f. przewalsii*	*Rh. sondaicus*
AR cumul	25	4.96	49.14	22.34	12.47	0.200	*Eq. f. przewalsii*	*T. bardii*

browser-grazers, and grazers. To determine the type of habitat and feeding, we used data from Sokolov (1979), Janis (1982), and Wilson and Mittermeier (2011).

Gambaryan (1974) identified six running forms in ungulates. In perissodactyls, Equidae were classified as cursorial runners, Rhinocerotidae as mediportal runners, and Tapiridae as battering-ram runners.

1. Cursorial form of running is an adaptation to life on open landscapes, characterized by the highest speeds and endurance (typical artiodactyl examples are reindeer, wildebeest, pronghorn, and saiga). Its distinctive features are a shallower trajectory (smaller take-off angles) of the center of gravity of the body in unsupported stages during gallop rather than during trot or pace, and the method of speed gain being mainly an increase of stride frequency compared to length.
2. Mediportal form of running is typical for large and heavy ungulates (e.g., bovines among artiodactyls). The vertical fluctuations of the center of gravity of the body are reduced compared to cursorial running form. The limb contact phase is characterized by decreased limb joint amplitudes and decreased pace angle (i.e. the angle by which the limb as a whole turns around the point of its contact with the ground).
3. Battering-ram form of running is typical for robust but not the largest forest ungulates (e.g., peccaries, hogs among artiodactyls). It is characterized by a steeper trajectory (larger take-off angles) of the center of gravity of the body in unsupported stages during gallop rather than during trot or pace. The limb contact phase is characterized by increased limb joint amplitudes and increased pace angle compared to the cursorial running form. The term "battering-ram" by itself implies low maneuverability.

4 | RESULTS

4.1 | Characteristics of vertebral column

The number of presacral vertebrae in perissodactyls is higher than in artiodactyls (29–32 vs. 25–27; mean 30.25 vs. 26.14) due to the higher number of thoracic vertebrae (Table 2). The number of presacral vertebrae in equids is, on average, higher than in rhinoceroses and tapirs (mean = 30.8 vs. 30.2 and 29.25) due to the higher number of lumbar vertebrae. The thoracic region in perissodactyls consists of 18–20 vertebrae, the lumbar region of 3–6 vertebrae (Tables S1 and S2). The maximum (20) of thoracic and the minimum (3) of lumbar vertebrae count is characteristic of rhinoceroses; the maximum number (6) of lumbar vertebrae is characteristic of equids. In artiodactyls, there are on average one more Tf than RfL joints (mean numbers are 10.1 vs. 8.94, respectively). In contrast, in perissodactyls, the number of Tf joints (mean = 17.59) is about 13 units greater than the number of RfL joints (mean = 4.93) the difference being significant ($Z = -4.555$, $p < 0.001$).

In perissodactyls, the length of the cervical region to the trunk (thoraco-lumbo-sacral) length ratio differs by two and a half times (Table 2). In equids the relative neck length (min = 40.9%, mean = 45.2%, max = 50.1%) is virtually the same as the mean in artiodactyls (44.8%). This ratio lies between the ratios of large antelopes, Cervidae, and small antelopes (mean = 40.8%, 41.9%, and

47.2%, respectively; Figure 4). Representatives of Rhinocerotidae (min = 28.1%, mean = 30.1%, max = 31.4%) and especially Tapiridae (min = 21.5%, mean = 23.4%, max = 25%) have very short necks (Figure 4). The relative length of the neck in tapirs and rhinoceroses is comparable to minimal ratios among even-toed ungulates found in Suina, Hippopotamidae, and Tragulidae (mean = 24.2%, 26.4%, and 28.9%, respectively).

The length of the thoracic region exceeds the length of the lumbar region, on average, more than threefold (Table 2, Figure 5). The relative length of lumbar region in Equidae (mean = 26.3%) and Tapiridae (mean = 21.3%) is similar to that of Giraffidae (mean = 25.2%) and Hippopotamidae (mean = 24.5%), which represent the minimum among artiodactyls. In Rhinocerotidae the lumbar region is even much shorter (mean = 14.1%; Figure 5).

The transition from the Rf to Tf type of zygapophysial joint in rhinoceroses almost always occurs at the first thoracic vertebra as in most even-toed ungulates. In equids and tapirs, it takes place at the second thoracic vertebra (except the rhinoceros-like T1 transition in *Tapirus terrestris* ZMMU S-93416).

The transition from Tf to RfL joint type in Equidae was found at the penultimate (in 13 of 16 specimens) or at the ultimate (in 3 of 16 specimens) thoracic vertebra. In tapirs and rhinoceroses, the transition either occurs at the penultimate (in 7 of 13 specimens), or at the ultimate (in 6 of 13 specimens) lumbar vertebra (Table S1). In the last case, only the lumbosacral joint shows RfL structure.

The number of Tf joints in perissodactyls is significantly higher than in artiodactyls (mean diff = 7.49), and the number of RfL joints is significantly lower (mean diff = −4.01). The Kruskal-Wallis

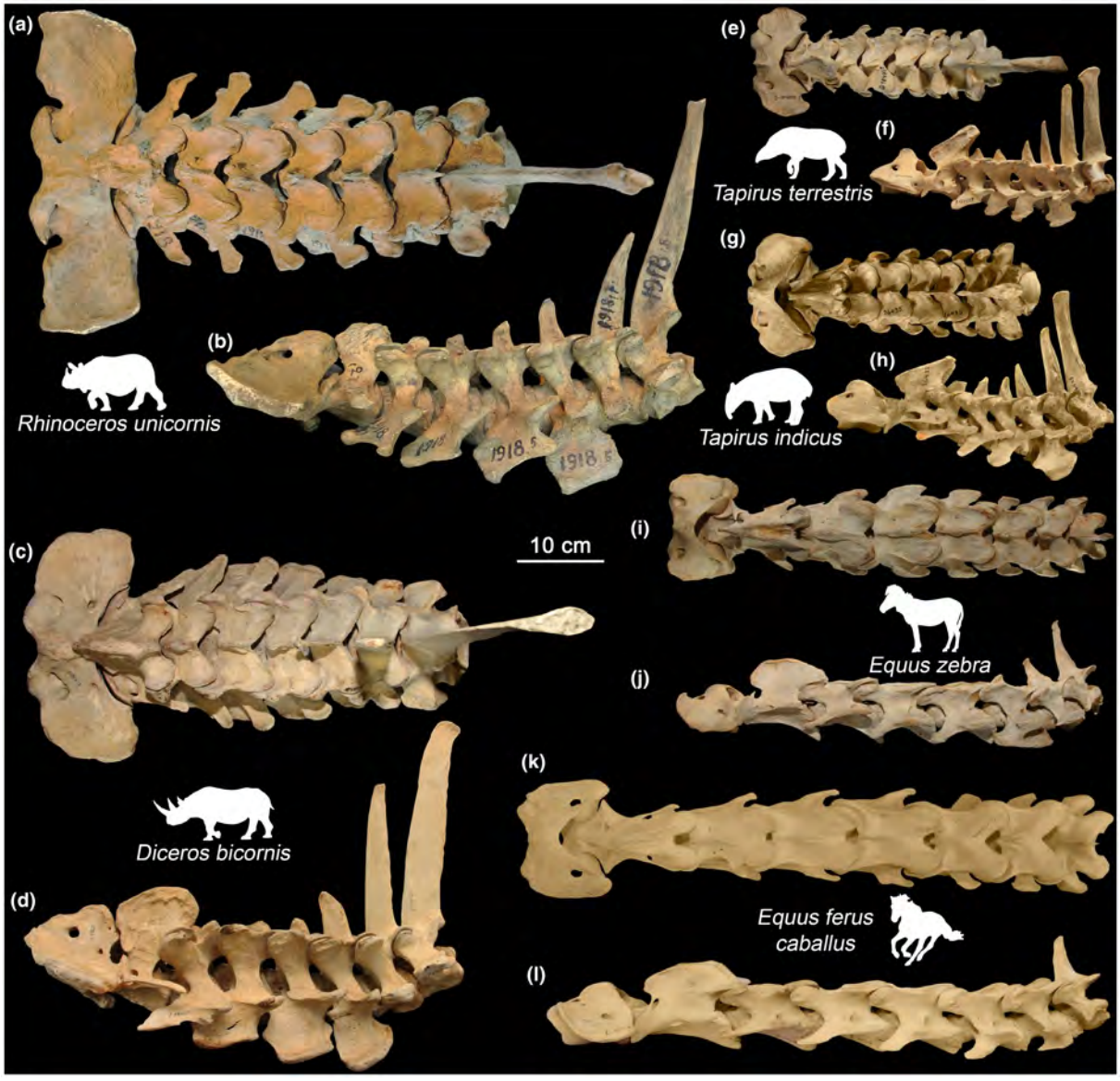

FIGURE 4 Cervical region (C1–T1) in various representatives of perissodactyls in dorsal (a, c, e, g, i, k) and left lateral (b, d, f, h, j, l) view. (a, b) *Rhinoceros unicornis* (ZIN 1918); (c, d) *Diceros bicornis* (ZMMU S-93020); (e, f) *Tapirus terrestris* (ZMMU S-184859); (g, h) *Tapirus indicus* (ZIN 26435); (i, j) *Equus zebra* (ZMMU S-105152); (k, l) *Equus ferus caballus* (ZMMU S-102019)

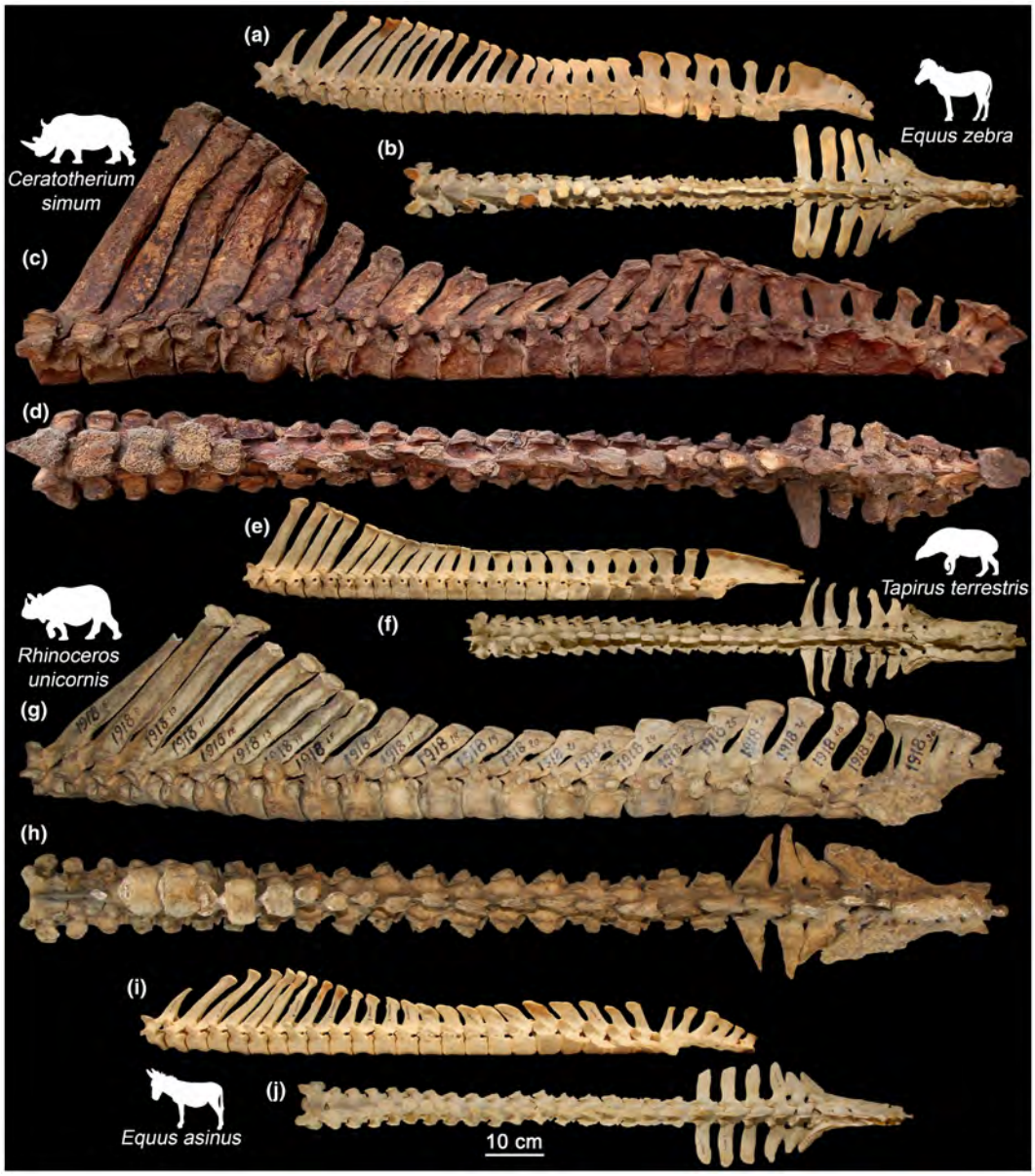

FIGURE 5 Thoracolumbar part of the backbone (T1–Sacrum) in various representatives of perissodactyls in left lateral (a, c, e, g, i), and dorsal (b, d, f, h, j) view. (a, b) *Equus zebra* (ZMMU S-105152); (c, d) *Ceratotherium simum* (RZ N/a); (e, f) *Tapirus terrestris* (ZMMU S-184859); (g, h) *Rhinoceros unicornis* (ZIN 1918); (i, j) *Equus asinus* (ZMMU S-74814)

H test indicates statistically significant differences among various groups of perissodactyls and artiodactyls in the number of both Tf ($\chi^2 = 69.840$, $p < 0.001$) and RfL joints ($\chi^2 = 63.670$, $p < 0.001$). Post Hoc Multiple Comparisons indicate that the group with the most numerous Tf and the fewest RfL joints includes Rhinocerotidae (***Tf***: mean = 20.75; ***RfL***: mean = 1.38) and Tapiridae (***Tf***: mean = 20.25; ***RfL***: mean = 2). By the number of Tf joints, Equidae (mean = 15.2) form a separate group between even-toed ungulates (mean numbers of different groups vary in the range from 8.83 to 12) and the rest of the perissodactyls (mean number is more than 20 Tf joints). By the number of RfL joints, Equidae (mean = 7.44) are between Giraffidae (mean = 6.67—minimal value in artiodactyls) and Bovini (mean = 7.86).

4.1.1 | Fusions in vertebral column

In contrast to artiodactyls (Belyaev et al., 2021b), a large number of cases of fusion between vertebrae with complete loss of mobility was observed in the studied perissodactyls (Figure 6). Fusions were observed in all regions of the vertebral column.

The only fusion in the cervical region was noted in Baird's tapir (Figure 6a,b). Fusion at the C2–C3 joint occurred both along the ventral side of the vertebral bodies and along the neural arches. It is interesting to note that in this individual there is a compensatory hypermobility in the next cervical joint. LB aROM in the C3–C4 joint (27.6°) is significantly higher than in other Rf joints C4–T2 (19.2–22.7°), and SB aROM in the C3–C4

FIGURE 6 Fusions in the vertebral column in perissodactyls in lateral (a, c, d, f, i), ventral (b, e, h, k) and dorsal (g, j) view. (a, b) C2–C3 of *Tapirus bardii* (ZMMU S-102033); (c–e) T3–T4 of *Ceratotherium simum* (NMW 3086); (f) T5–T6 of *Ceratotherium simum* (RZ N/A); (g, h) L5–L6 of *Equus ferus przewalskii* (ZMMU S-158572); (i) T15–T16 of *Equus asinus* (ZMMU S-74814); (j, k) L5-L6 of *Equus ferus caballus* (ZMMU S-106944)

joint (15.3°) is the largest in the Rf division among all the tapirs studied (Table S2).

In the Tf division, fusions were observed in both white rhinoceroses: on the ventral side of the vertebral bodies and the upper part of the spinous processes at T3–T4 (NWM 3086) (Figure 6c–e) and in the form of a large traumatic overgrowth on the ventral side of the vertebral bodies at T5–T6 (RZ N/A) (Figure 6f). In *Equus asinus* (ZMMU S-74814) there was an extensive fusion between spinous processes of four posterior thoracic vertebrae (T15–T18) (Figure 6i).

In the RfL division, fusions were found between transverse processes at L4–L5 in a kulan (ZMMU S-102029), between transverse processes and on the ventral side of the vertebral bodies at L5–L6 in a pony (ZMMU S-106944) (Figure 6j,k), and between transverse processes at L5–L6 in Przewalski's horse (ZMMU S-158572) (Figure 6g,h).

A large number of pathologies described above can be associated with the effects of keeping most of the studied animals in captivity, lack of activity, and age-related changes (Gunji et al., 2014; O'Regan & Kitchener, 2005). However, most of the artiodactyls we studied earlier (Belyaev et al., 2021b) were animals kept in captivity as well, but they were characterized by a notably smaller number of fusions between vertebrae with complete loss of mobility (7 of 30 specimens in perissodactyls, 3 of 54 specimens in artiodactyls).

4.2 | Rf division

The K–S test showed that the mobility in the joints of the cervical region in our sample does not have a normal distribution (***SB***: $n = 195$, $p = 0.016$; ***LB***: $n = 169$, $p = 0.004$). The Fisher-Pearson coefficient of

skewness (***SB***: −0.030; ***LB***: −0.682) indicated that the distribution is skewed left, toward lower aROM values (due to tapirs and rhinoceroses). In contrast to the artiodactyls, aROM values in the joints of the cervical region in perissodactyls are almost evenly distributed (Figure 7). The Kruskal–Wallis *H* test indicated that the differences in mean aROM values in joints are statistically significant only in LB (***SB***: $\chi^2 = 5.489$, $p = 0.483$; ***LB***: $\chi^2 = 37.403$, $p < 0.001$). Post Hoc Multiple Comparisons indicated that mean SB aROMs in Rf joints are not significantly different (min = 11.1°, mean = 12.4°, max = 13°). However, the mean ranks in the neck-thorax (C7–T1) and first intrathoracic (T1–T2) joints (***LB***: 57.98 and 37.43 respectively) were noticeably lower than those in the C2–C7 joints (***LB***: 91.93–108.17). Post Hoc Multiple Comparisons distinguished two or three homogeneous groups among the joints of the cervical region when considering LB aROM. Joints C2–C7 belong to the subset with higher LB aROMs (mean values range from 26.9° to 29.3°) and C7–T2 joints belong to the subset with lower LB aROMs (mean values 24.2° and 21.7°) (Figure 7b).

In equids and the majority of tapirs (4 of 5 specimens), the first intrathoracic joint (T1–T2) has Rf facet type, like in the neck. Student's *t*-test (independent samples) showed that the mean aROM in the T1–T2 joint in these specimens of equids and tapirs is slightly

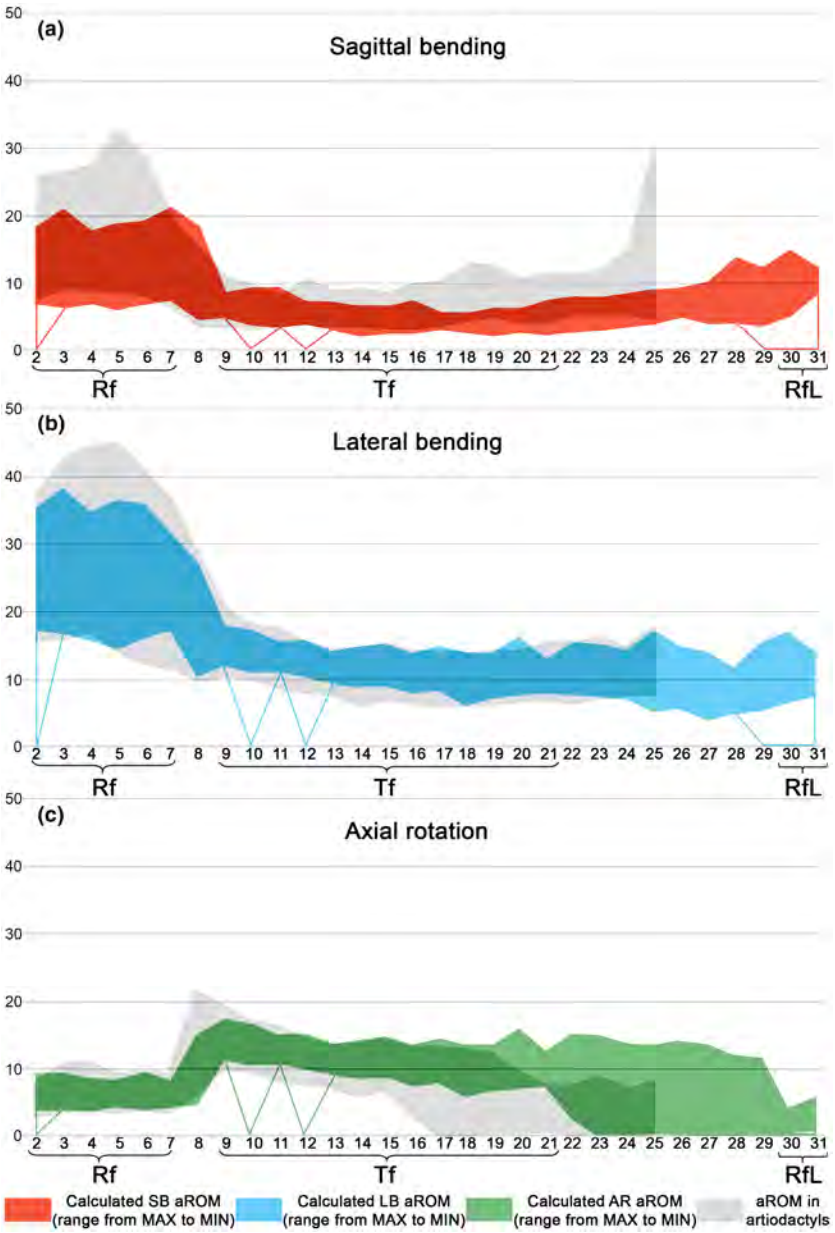

FIGURE 7 aROM variability (range from maximum to minimum) in the presacral intervertebral joints in perissodactyls. (a) SB aROM; (b) LB aROM; (c) AR aROM. Abscissa axis is graduated by joint numbers. The lines dropping down to zero by vertical axis indicate vertebral fusions. For comparison, aROMs previously reported for artiodactyls (Belyaev et al., 2021b, 2022) are shown as the grey zone.

smaller compared to the neck-thorax joint (C7–T1) joint in SB (mean diff = −2.6°, t = −2.707, p = 0.010, 95% CI: −4.5° to −0.6°) and LB (mean diff = −3.2°, t = −3.185, p = 0.003, 95% CI: −5.2° to −1.2°).

4.2.1 | Sagittal bending aROM

The cumulative SB aROM in the Rf division varies by more than 60° across perissodactyls (Table 3). The Mann–Whitney U test shows that cumulative SB aROM in perissodactyls is not significantly lower than in artiodactyls (U = 597, p = 0.096, mean diff = −10.2°). The Kruskal–Wallis H test indicated statistically significant differences between groups of odd-toed and even-toed ungulates (χ^2 = 63.50, p < 0.001). Post Hoc Multiple Comparisons indicated that Rhinocerotidae (57.4°) and Tapiridae (66.6°) form the group with the lowest SB aROM; cumulative SB aROM in pigs, hippos, and bovins is somewhat higher (mean 74.3°, 75.5°, and 80.3°, respectively; Figure 8a). Equidae have higher-than-average values (mean = 101.7°) of the cumulative SB aROM in the cervical region, similar to that of large antelopes, Tragulidae, and Tayassuidae (mean 94.8°, 101.1°, and 105°; Figure 8a). However, this value is markedly lower than in Camelidae and Giraffidae (mean 122.1° and 128.3°, respectively).

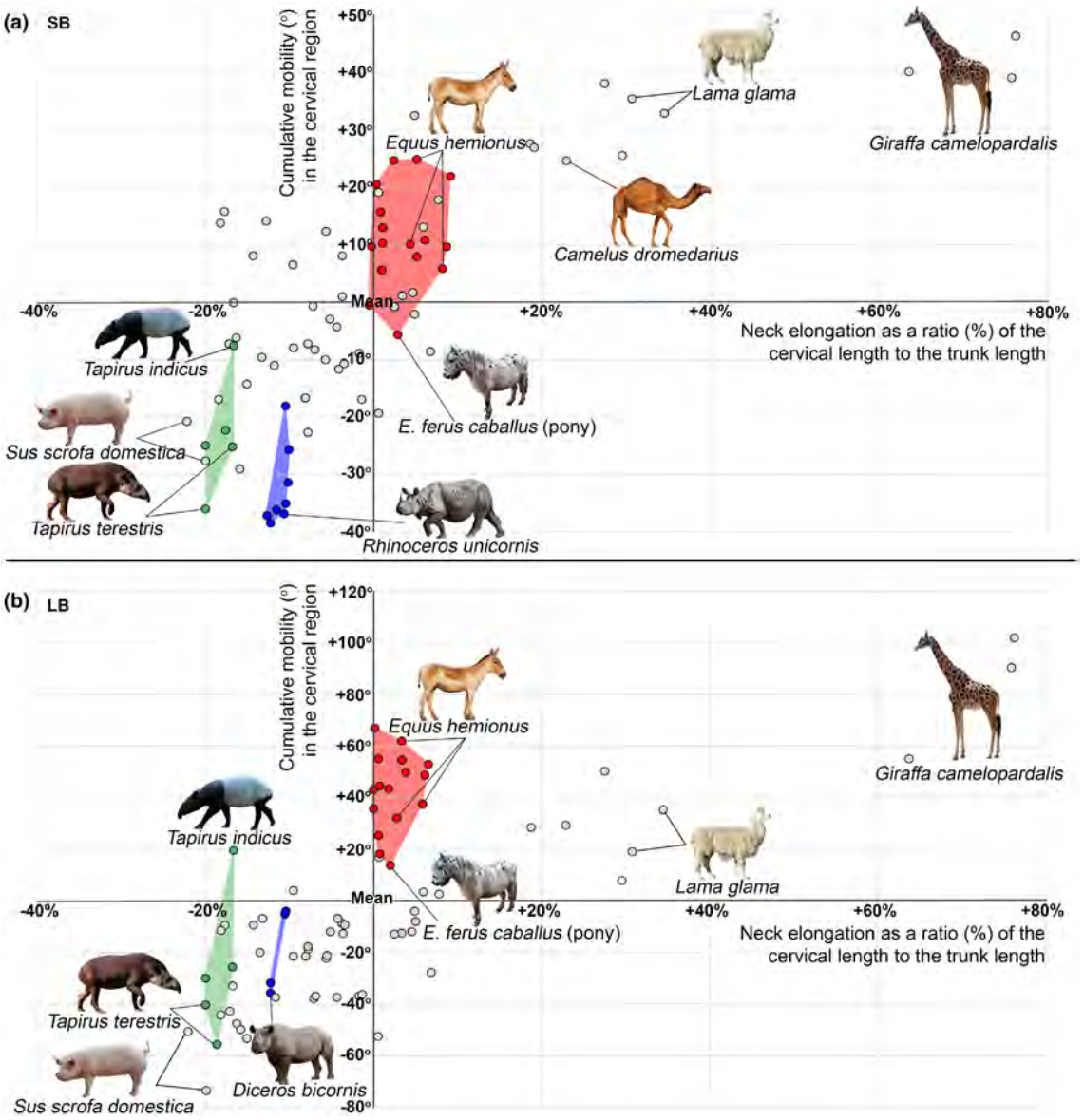

FIGURE 8 Mobility in the cervical region in perissodactyls. (a) SB aROM; (b) LB aROM. Abscissa axis represents the neck elongation as a percentage (%) of the cervical length to the trunk length (T + L + S). Ordinate axis represents the cumulative mobility (°) in the cervical intervertebral joints. Mean values for all studied odd-toed and even-toed ungulate species are taken for the point of axes intersection (neck elongation mean = 41.66%; cumulative SB aROM mean = 90.05°; cumulative LB aROM mean = 155.51°). The circle colors indicate the taxonomic group: Equidae (red), Rhinocerotidae (blue), Tapiridae (green). Grey circles indicate data previously reported for artiodactyls (Belyaev et al., 2021b). The list of the studied artiodactyls is given in Table S1.

4.2.2 | Lateral bending aROM

The range of cumulative LB aROM in the Rf division varies by more than 100° across perissodactyls (Table 3). The Mann–Whitney *U* test shows that cumulative SB aROM in perissodactyls is statistically significantly higher than in artiodactyls ($U = 347$, $p = 0.001$, mean diff = 28.4°). The Kruskal–Wallis *H* test indicated statistically significant differences between groups of odd-toed and even-toed ungulates ($\chi^2 = 62.472$, $p < 0.001$). Post Hoc Multiple Comparisons indicated that Tapiridae (mean = 136.7°) and Rhinocerotidae (mean = 143.7°) have cumulative LB aROMs similar to that of Bovini (mean = 150.1°; Figure 8b). A markedly lower LB aROM is characteristic of Hippopotamidae (mean = 119.1°) and Suina (mean = 123.8°). Equidae (mean = 205.4°) are second only to giraffes in cumulative LB aROM (mean 205.4° vs. 246.5° in Giraffidae). It is worth noting that Equidae have the same number of Rf joints as giraffes (7) and one more Rf joint than the majority of ungulates including Camelidae.

4.2.3 | Axial rotation aROM

The variability of the cumulative AR aROM across perissodactyls is within 25° (28.6–50.75°) (Table 3, SuppInfo Table S2, Figure 7c). Student's *t*-test (independent samples) shows that cumulative AR aROM in perissodactyls is statistically significantly higher than in artiodactyls (mean diff = 5.0°, $t = 3.348$, $p = 0.002$, 95% CI: 2.0 to 8.0°). ANOVA indicates a statistically significant difference in cumulative aROMs in various groups of odd-toed and even-toed ungulates ($F = 7.994$, $p < 0.001$). Post Hoc Multiple Comparisons separated Equidae as a group with slightly higher AR aROM (mean = 43.8°).

4.3 | Tf division

Student's *t*-test (paired samples) showed that the mean aROMs in the joints of the anterior half of the Tf division are slightly, but significantly, greater than aROMs in the posterior half of the Tf division in all three directions of mobility (***SB***: $n = 21$, mean diff = 0.6°, $t = 3.504$, $p = 0.002$, 95% CI: 0.3° to 1.0°; ***LB***: $n = 17$, mean diff = 1.4°, $t = 4.292$, $p = 0.001$, 95% CI: 0.7° to 2.1°; ***AR***: $n = 17$, mean diff = 1.3°, $t = 4.197$, $p = 0.001$, 95% CI: 0.7° to 2.0°).

4.3.1 | Sagittal bending aROM

The cumulative SB aROM in the Tf division varies by 60° across perissodactyls (Table 4, Table S2, Figure 7a). The Kruskal–Wallis *H* test indicates statistically significant differences between groups of odd-toed and even-toed ungulates in SB aROM in the posterior half of the thoracic region ($\chi^2 = 41.500$, $p < 0.001$). Mean SB aROM in the posterior half of the thoracic region in Equidae (4.5°) and Rhinocerotidae (4.6°) are the lowest among all families of odd-toed and even-toed ungulates. For comparison, the largest mean SB aROM in the posterior half of the Tf division is characteristic of Tragulidae (8.2°).

ANOVA indicates that the cumulative SB aROMs in the Tf division in odd-toed and even-toed ungulates groups differ significantly ($F = 22.897$, $p < 0.001$). Rhinocerotidae (mean = 103.5°) and Tapiridae (mean = 107.5°) form the subset with the highest cumulative SB aROM. Equidae (mean = 75.7°) are markedly lower in cumulative SB aROM and are closest to Bovini (mean = 65.5°).

4.3.2 | Lateral bending and axial rotation aROMs

The cumulative LB and AR aROMs in the Tf division varies by ~90° across perissodactyls (Table 4). The Mann–Whitney *U* test indicates that mean LB and AR aROMs in Tf joints in perissodactyls and artiodactyls do not differ significantly (***LB***: $U = 321$, $p = 0.161$; ***AR***: $U = 335$, $p = 0.276$). The number of Tf joints in perissodactyls significantly exceeds that of artiodactyls, and thus the cumulative LB and AR aROMs of odd and even-toed ungulates differ by more than 80° (***LB***: $t = 14.469$, $p < 0.001$; ***AR***: $t = 14.755$, $p < 0.001$).

4.4 | Lumbar region including lumbosacral joint

4.4.1 | Sagittal bending aROM

The cumulative SB aROM varies 40° across perissodactyls (Table 5). ANOVA indicates that the SB aROMs in the lumbar region (including the lumbosacral joint) in the groups of odd-toed and even-toed ungulates are significantly different both in cumulative ($F = 17.994$, $p < 0.001$) and mean values ($F = 6.583$, $p < 0.001$). According to Post Hoc Multiple Comparisons, all three families of perissodactyls belong to the group with the lowest mean SB aROMs (mean values range from 7.1° to 7.7°) along with such large artiodactyls as Giraffidae, Bovini, and Hippopotamidae (mean values range from 7.5° to 8.4°; Figure 9). The cumulative lumbar SB aROM is also low, with rhinoceroses characterized by the lowest values (mean = 29.6°) across all studied odd-toed and even-toed ungulates. Tapirs are on average 10° greater than rhinoceroses and are close to Giraffidae and Hippopotamidae showing the minimum cumulative lumbar SB aROM values among artiodactyls (mean values 42.2°). Equidae are on average 10° greater than Tapiridae and have the same cumulative SB aROM as bovines being on average 10° less than large antelopes (Figure 9).

Student's *t*-test (paired samples) showed that the mean SB aROMs in the lumbar Tf joints in tapirs and rhinoceroses are significantly higher than in the posterior half of the thoracic Tf joints ($n = 11$, mean diff = 1.4°, $t = 3.82$, $p = 0.003$, 95% CI: 0.6° to 2.1°) (Figure 7a).

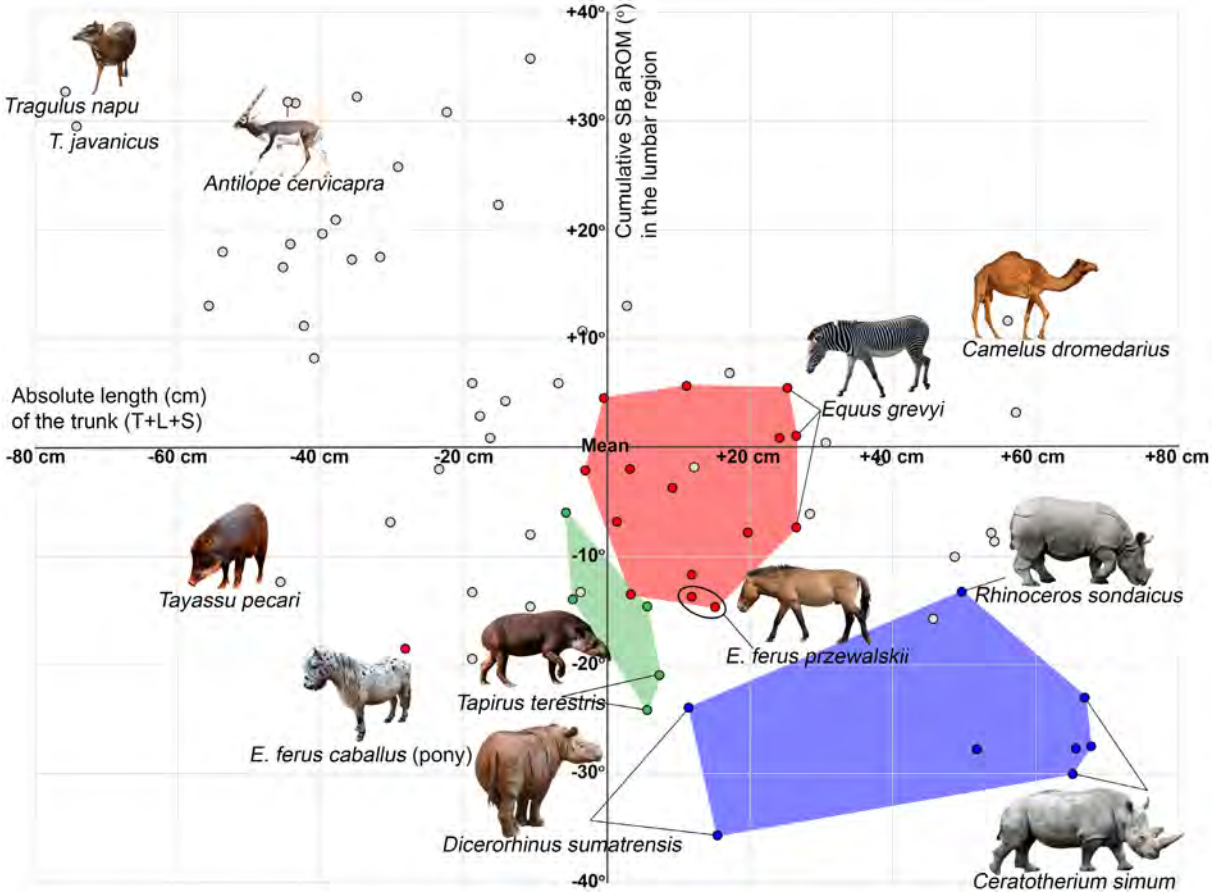

FIGURE 9 Sagittal mobility in the lumbosacral part of the backbone in perissodactyls. Abscissa axis represents the absolute length (cm) of the trunk (T+L+S). Ordinate axis represents the cumulative SB aROM (°). Mean values for all studied odd-toed and even-toed ungulate species are taken for the point of axes intersection (trunk length mean = 101.3 cm; cumulative SB aROM in lumbar region together with the lumbosacral joint mean = 55.71°). Circle colors indicate taxonomic groups as in Figure 8.

Student's *t*-test (independent samples) shows that Equidae have significantly lower cumulative SB aROM in the lumbar region than artiodactyls employing the same cursorial running form (mean diff = −12.7°, $t = -3.264$, $p = 0.007$, 95% CI: −21.3° to −4.2°), Tapiridae have significantly lower cumulative SB aROM than the similarly battering-ram-running Suina (mean diff = −19.7°, $t = -3.970$, $p = 0.003$, 95% CI: −30.7° to −8.6°), and Rhinocerotidae have significantly lower cumulative SB aROM than the similarly mediportal-running Bovini (mean diff = −20.8°, $t = -6.762$, $p < 0.001$, 95% CI: −27.5° to −14.2°).

The cumulative SB aROM in the RfL division is highly variable due to the difference in the number of RfL joints. Because of the strongly reduced number of RfL joints (1–2), the cumulative SB aROM in Rhinocerotidae (mean = 12.7°) and Tapiridae (mean = 20.6°) is significantly lower than in any of the even-toed ungulates (the minimum SB aROM is characteristic of Giraffidae (mean = 49.8°)). The cumulative SB aROM in Equidae (mean = 56.4°) slightly exceeds Giraffidae and is closest to Bovini (mean = 58.8°). It is also worth noting that the lowest mean SB mobility in RfL joints among all of studied ungulates are characteristic of the pony (ZMMU S-106944, mean = 5.2°) and both studied Przewalski's horses (5.8° and 5.9°).

4.4.2 | Lateral bending aROM

The cumulative LB aROM in the lumbar region (including lumbosacral joint) varies 35° across perissodactyls (Table 5). ANOVA indicates that the LB aROMs in the lumbar region (including the lumbosacral joint) in the groups of odd-toed and even-toed ungulates are statistically significantly different both in cumulative ($F = 7.809$, $p < 0.001$) and mean values ($F = 5.141$, $p < 0.001$). Equidae are characterized by lowest mean LB aROM in the lumbar region joints (8.6°). The lowest cumulative LB aROMs in the lumbar region is found in Rhinocerotidae (mean = 46.8°) and Hippopotamidae (mean = 45.2°). Equidae (mean = 57.3°) and Tapiridae (mean = 57.7°) are characterized by somewhat higher cumulative LB aROMs on a par with Giraffidae (mean = 56.7°).

4.4.3 | Axial rotation aROM

In Equidae, the cumulative AR aROM is low (mean = 15.3°) and close to that of Suidae, Cervidae, and Caprinae (mean = 13.3°, 16°, and 17.6°, respectively). In Rhinocerotidae and Tapiridae, due to Tf facets, both mean (6.6° and 7.7°, respectively) and cumulative

(mean = 33.3° and 36.1°, respectively) AR aROMs in the lumbar region are the highest among ungulates.

5 | DISCUSSION

5.1 | Shifts of facet-type transitions

5.1.1 | Transition from radial to tangential facets

In almost all artiodactyls, the Rf-Tf transition (from radial to tangential type of zygapophysial facets) occurs at the first thoracic vertebra (T1) (Belyaev et al., 2021b). The same is true for rhinoceroses, but in equids and tapirs this transition occurs at the second thoracic vertebra (T2), like in giraffes. Therefore, in these perissodactyls, T1–T2 joint has Rf-type zygapophyses, like in the neck. The intervertebral disc in the T1–T2 joint in domestic horse is, on average, more than twice as thick as the intervertebral discs in the rest of the thoracic joints (Townsend & Leach, 1984). The experimentally measured SB aROM in the T1–T2 joint in horses is more than three times higher than that in the next thoracic joints (Townsend et al., 1983). A similar specialization of the T1–T2 joint was shown for the giraffe (Gunji & Endo, 2016). Our data show that in SB aROM the T1–T2 joint in all perissodactyls together (including rhinoceroses with Tf type of this joint) is, on average, only slightly less mobile than the other Rf joints (by 1.9–3.0°) and significantly more mobile than thoracic Tf joints beginning with T2–T3 (by more than 5°). In LB aROM, the T1–T2 joint is on average 2.4° less mobile than the neck-thorax connection (C7–T1 joint), and 5.2–8.5° less mobile than the intracervical joints. Specialization of the first intrathoracic joint provides the equid neck with extra mobility, making it an even more agile manipulator, like in giraffe. The functional role of Tf-to-Rf transformation of the T1–T2 joint in tapirs is not as clear.

5.1.2 | Transition from tangential to radial with a lock facets

In artiodactyls, the posterior part of the thoracic region is the place of transition from Tf to RfL type of zygapophysial joints (Belyaev et al., 2021b). Unlike artiodactyls, in perissodactyls, the posterior part of the thoracic region retains Tf joints (Figure 1c–f), with the exception of some Equidae, which posterior-most intrathoracic joint facets are shaped as RfL. Overall, rhinoceroses and tapirs have few RfL joints (mean 1.38 and 2, respectively), equids have 6–9 RfL joints, and artiodactyls have 6–12 RfL joints. In the early Eocene equoid *Arenahippus grangeri* (UM 115547; formerly *Hyracotherium grangeri*), Tf to RfL transition occurred at T15 (the last thoracic vertebrae being T17; Wood et al., 2011), so this equoid had 10 RfL joints including two intrathoracic, one thoracolumbar, six intralumbar, and one lumbosacral. This indicates that the significant reduction in the number of RfL joints in favor of Tf joints is, probably, a derived feature of rhinoceroses and tapirs. It should be emphasized, that the RfL-to-Tf replacement reduces SB aROM but automatically increases AR aROM. This gives an additional advantage in increasing the ability to tilt hindquarters relative to forequarters during maneuvering, although its importance in tapirs and rhinoceroses is doubtful.

Among perissodactyls, the zygapophysial joints of the lumbar region have an RfL geometry only in representatives of Equidae family (Figure 10e,f). The 'locks' of the 'Radial facet with a Lock' (RfL) in Equidae are shaped very simply compared to those of artiodactyls: the prezygapophyses completely lack dorsal ridges enclosing the postzygapophyses of the previous vertebra in even-toed ungulates (see Figure 10g–l). The morphology of the lumbar zygapophyses in tapirs and rhinoceroses, are even more simplistic than in Equidae and are similar to Rf type of the cervical joints. In Tapiridae and Rhinocerotidae only the posteriormost intralumbar and lumbosacral joints are characterized by U-like (RfL type) or the simpler V-like (Rf type) shape in the transverse plane (Figure 10a–d), while the majority of the intralumbar joints, anterior ones, have the Tf type of zygapophysial facets. In other words, in tapirs and rhinoceroses the Tf-to-RfL transition occurs in the lumbar region, while in artiodactyls it is found in the thoracic region. Thus, in perissodactyls, only representatives of the Equidae family have RfL joints throughout the lumbar region (Figure 10), like artiodactyls. The RfL joints almost completely exclude AR in favor of SB involved in galloping.

5.2 | Cervical region

The neck of perissodactyls (as well as artiodactyls) is the main manipulator for interacting with the habitat, as the arm in humans. The cervical region is the most mobile region of the presacral vertebral column in terms of SB and LB aROM: Mean SB and LB aROM values in the Rf joints (12.4° and 26.9°, respectively) significantly exceed those in the Tf (5.0° and 11.5°, respectively) and RfL joints (8.4° and 9.3°, respectively). Mean LB aROM (26.9°) in the Rf joints more than twice exceeds mean SB aROM (12.4°); in even-toed ungulates this disproportion is much lower (25.0° vs. 15.3°) (Belyaev et al., 2021b). Apparently, this is due to smaller R_{lat} and larger R_{vert} (see Figure 3), relative to zygapophysial facets' dimensions, in perissodactyls than in artiodactyls. Increased LB aROM in the neck may be beneficial in respect of grooming the flanks of the body.

In various artiodactyls the length of the cervical region relative to trunk length differs almost sixfold (Belyaev et al., 2021b). The neck length separates extant perissodactyls into just two groups (Figure 8). The relative length of the neck in tapirs and rhinoceroses is comparable to minimal ratios among even-toed ungulates found in Suina, Hippopotamidae, and Tragulidae. In Equidae, the relative neck length is at the average level of artiodactyls and closest to that of Cervidae, large and small antelopes (mean from 40.8% to 47.2%). Probably, the neck elongation conforms the leg elongation allowing to reach ground or water when feeding and drinking with straight forelimbs.

Data from Clayton and Townsend (1989a, 1989b) show that a significant proportion of the cervical mobility is located in two synovial

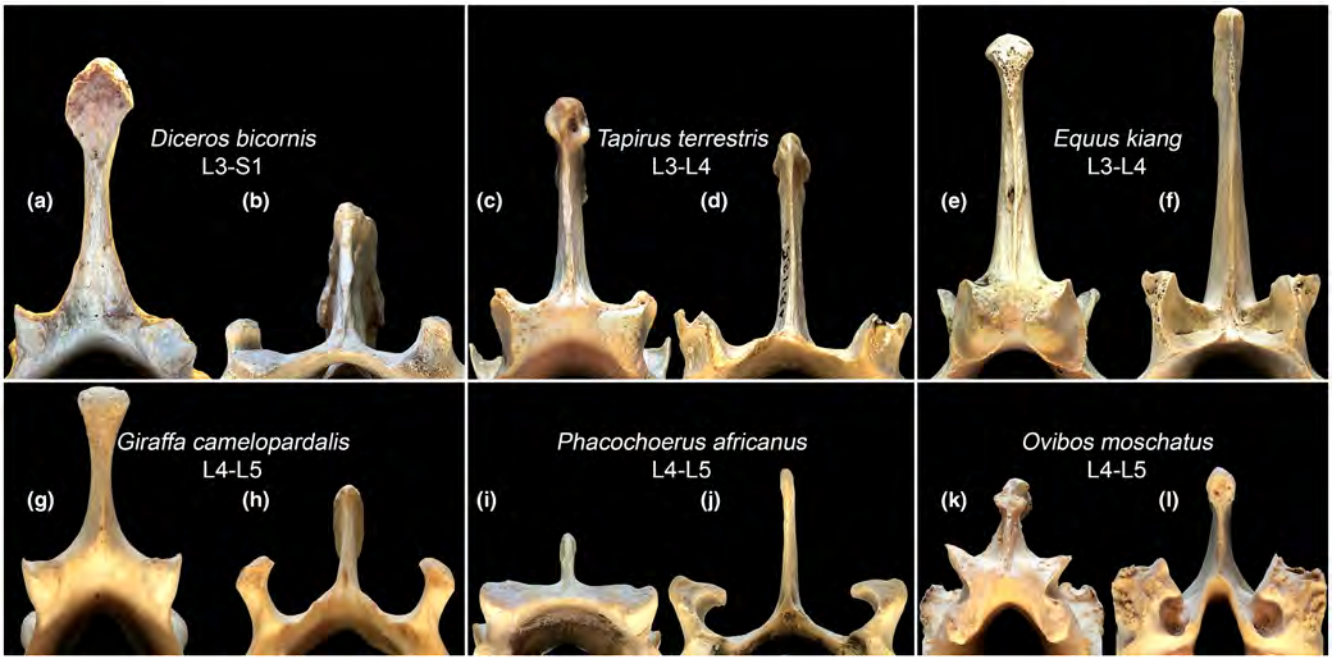

FIGURE 10 The geometry of zygapophysial locks in the RfL joints of various ungulates: Posterior view of postzygapophyses of an anterior vertebra in a pair (a, c, e, g, i, k) and anterior view of corresponding prezygapophyses of a posterior vertebra in a pair (b, d, f, h, j, l). The examples are displayed in a sequence of increased lock closure. (a, b) *Diceros bicornis* (ZMMU S-93020); (c, d) *Tapirus terrestris* (ZMMU S-184859); (e, f) *Equus kiang* (ZMMU S-166817); (g, h) *Giraffa camelopardalis* (ZMMU S-175340); (i, j) *Phacochoerus africanus* (ZMMU S-171945); (k, l) *Ovibos moschatus* (ZMMU S-135832)

joints: the occipital and the atlas-axis joints. These two joints account for 93% of the cumulative AR (mean = 26.9° in the occipital joint, mean = 107.5° in C1–C2), 38.6% of the cumulative SB (86.4° and 16.2°, respectively), and 20% of the cumulative LB (43.9° and 3.9°, respectively) of the cervical region. Thus, SB and LB aROMs are maximal in the occipital joint, while AR aROM in the C1–C2 joint.

In artiodactyls the posterior neck joints (C4–C7) are significantly more mobile (on average by 2.5–3.5°) as compared to anterior joints (C2–C4) and to the neck-thorax joint (C7–T1) in SB and LB (Belyaev et al., 2021b). In perissodactyls, mobility is almost evenly distributed in the post-axis cervical region. Only the LB aROM of the neck-thorax joint is significantly less mobile (on average by 2.7–5.1°) than the LB aROM of the intracervical joints.

Rhinoceroses and tapirs are ungulates with the least mobile neck in the sagittal plane; cumulative SB aROM is lower than that of pigs, hippos, and bovins (Figure 8a). However, the cumulative LB aROM in rhinoceroses and tapirs (mean ~ 140°) is markedly higher compared to the minimal values in artiodactyls such as in pigs and hippos (mean ~ 120°; Belyaev, 2018; Belyaev et al., 2021b; Wilke et al., 2011; Figure 8b). Compared to artiodactyls, the cumulative SB aROM in the cervical region of Equidae (mean = 101.7°) is higher-than-average, being similar to that of large antelopes. The cumulative LB aROM of Equidae (mean ~ 200°) is only lower than in giraffes, being on a par with camels and llamas (mean ~ 190°; Belyaev et al., 2021b; Stolworthy et al., 2015). Our calculated LB aROM for the neck of domestic horse and the experimental values obtained in vitro by Clayton and Townsend (1989a, 1989b) almost coincide (on average 32.3° vs. 31.9°, respectively). However, the cervical SB aROM of domestic horses from the same experiments is considerably higher than provided by our calculations for Equidae and reach 87% of LB as opposed to our estimate of 49% (Figure S3). The data from Clayton and Townsend (1989b) can be used for adjustment of K_S and K_R coefficients in the formula for more precise calculation of SB aROMs in Rf joints of Equidae (Table S3.1); the recalculated SB aROM values are presented in Table S3.2. However, this adjustment is hardly applicable to the neck SB mobility calculation for tapirs and rhinoceroses.

The relatively short neck is an ancestral state for perissodactyls. Based on measurements from Cope (1873) the relative neck length in the small Paleogene rhinocerotoid *Hyrachyus eximius* was 19.7% of the trunk length. Based on measurements from Wood et al. (2011) and 3D skeleton from UMORF website (https://umorf.ummp.lsa.umich.edu/wp/specimen-data/?Model_ID=1675) the relative neck length in the *A. grangeri* was 23.5% of the trunk length. This is similar to the lowest ratios of extant odd-toed and even-toed ungulates. We have roughly calculated aROM values for the C5-C6 joint of *Arenahippus* based on the low-resolution 3D models from the UMORF: ***SB***: 13.3°, ***LB***: 21.2°. Extrapolating these values to all joints of the Rf division, the cumulative aROM should have been 79.8° in SB and 127.2° in LB. These values are slightly higher than in rhinoceroses and tapirs in SB, and, on the contrary, slightly lower in LB. Thus, both relative length of the neck and the intervertebral bending mobility in the cervical joints in basal equoids were significantly lower than in modern-day equids.

To summarize, the neck of perissodactyls is characterized by a significant prevalence of LB over SB mobility (2.17-fold), which is

considerably higher than was earlier reported for artiodactyls (1.63-fold; Belyaev et al., 2021b), and significantly higher than in domestic cats and humans (LB ≈ SB; Jones et al., 2020; Wen et al., 1993). The relatively short neck of rhinoceroses is characterized by low mobility. Stiffness of the neck of rhinoceroses is probably associated with the heavy head, which is used for fighting (Wilson & Mittermeier, 2011). In contrast, the relatively long neck of equids performs a primarily manipulative function. The equid neck is characterized by rather high bending mobility (especially LB) and is functionally elongated by the first thoracic joint (T1–T2), which is characterized by significantly increased bending mobility due to the neck-like Rf (instead of Tf) articulation.

5.3 | Spine stiffness and gallop in odd-toed ungulates

5.3.1 | Thoracic region

The SB aROM in the Tf division is markedly smaller compared to that of the Rf division (on average 5.0° vs. 12.4°). The anterior part of the thoracic region (the withers) in ungulates shows size-dependent reinforcement, including an impressive lengthening of the spinous processes of the vertebrae. This reinforcement helps to carry the weight of the heavy head, neck, and thorax, especially during the forelimb support stage while galloping (Gambaryan, 1974). The spinous processes of the withers are the attachment area of nuchal ligament that stores and recovers elastic energy during vertical oscillations of the head. In a walking horse, the nuchal ligament allows recovery of up to 60% of this energy (Gellman & Bertram, 2002).

The number of presacral vertebrae in perissodactyls is significantly higher ($p < 0.001$, mean diff = 4.11) than in artiodactyls (29–32 vs. 25–27) due to the higher number of thoracic vertebrae. This increased number was acquired convergently with afrotherians (Narita & Kuratani, 2005; Sánchez-Villagra et al., 2007). The large number of presacral (more specifically, thoracolumbar) vertebrae is probably the ancestral state for the odd-toed ungulates, as the early Eocene *A. grangeri* and middle Eocene *Mesohippus bairdi* (AMNH 1477) already had 31 presacral vertebrae (Scott et al., 1941; Wood et al., 2011). Both Paleogene equoids mentioned are characterized by the vertebral formula 7C + 17T + 7L. The common vertebral formula of extant equids is 7C + 18T + 6L with relatively frequent deviation 7C + 18T + 5L and relatively rare deviations 7C + 17T + 6L, 7C + 17T + 7L, 7C + 18T + 7L, 7C + 19T + 5L, and 7C + 19T + 6L (Spoormakers et al., 2021; Table S1 herein). Extant rhinoceroses and tapirs are characterized by a further increased number of thoracic vertebrae (18–20 and 18–19, respectively) at the expense of a reduced number of lumbar vertebrae. For example, there are 7 lumbar vertebrae in the small Eocene rhinocerotoid *H. eximius*, 5 in the relatively large (~0.5 m skull, ~2 m long) Late Eocene *Trigonias osborni* (Scott et al., 1941), and 3–4 in extant rhinoceroses. This change of balance in favor of thoracic vertebrae is probably associated with homeotic effects produced by shifts in the expression of homeobox genes controlling the anteroposterior axial regionalization (Iimura et al., 2009).

Mean SB aROMs in the posterior half of the thoracic region in Equidae and Rhinocerotidae are the lowest among all families of odd-toed and even-toed ungulates. At first sight, it may seem contradictory that perissodactyls, compared to artiodactyls, have reduced SB mobility in the intrathoracic joints but an increased number of thoracic vertebrae. The seeming discrepancy between reduced mobility and increased vertebral number in the perissodactyl thorax has an apparent functional explanation. One of the most prominent and acknowledged morpho-physiological features of perissodactyls is hindgut fermentation of cellulose, as opposed to foregut fermentation in artiodactyls. The increased number of vertebrae lengthens the perissodactyl thorax to fit an enlarged hindgut. At the same time, the posterior thoracic part of the vertebral column, stiffened due to reduced SB aROM of Tf joints, is able to passively support the hindgut heavily loaded with roughage against sagging down in the sagittal plane. A converse example of the interrelation between the digestive system and the regionalization of vertebral column mobility is found in Suidae. These animals do not have chambered stomachs or enlarged caeca and cannot digest cellulose efficiently (Wilson & Mittermeier, 2011). Their backbone is characterized by the largest, among artiodactyls, number of RfL joints in the posterior part of the thoracic region (mean = 3.8; Belyaev et al., 2021b). As a result, this part of suid thoracic region is characterized by increased SB amplitudes compared to those in the middle third (Tf joints) of the thoracic region (Busscher et al., 2010; Wilke et al., 2011).

5.3.2 | Lumbar region

The adaptation of quadrupedal mammals to gallop involves, among other features, an ability of the lumbar region of the vertebral column to flex and extend in the sagittal plane. For example, studies of backbone kinematics in horses show that these animals actively engage SB of the lumbar region only during bounding gaits (represented in the experiments not by gallop but by canter) (Faber et al., 2001b; Haussler et al., 2001), and barely use it when walking and trotting (Faber et al., 2000; Haussler et al., 2001). Sagittal flexion and extension of the backbone, synchronized with respective actions of the hindlimbs, allow quadrupedal mammals to increase the hindlimb range of motion (Hildebrand, 1959). Storage and recoil of elastic energy in the *m. longissimus thoracis et lumborum* aponeurosis allow mammals to reduce metabolic cost of gallop and make this gait most energy efficient at high speeds (Alexander et al., 1985).

The difference in gallop performance between the most studied ungulates and the carnivores is so pronounced that Gambaryan (1974) opposed them as “the dorsostable runners” and “the dorsomobile runners,” respectively. Contrary to this opposition, in our previous studies, we have shown that SB mobility of the backbone varies in even-toed ungulates from restricted to high (Belyaev et al. 2021b, 2022). In various small and medium-sized artiodactyls that use the saltatorial and saltatorial-cursorial running forms (Tragulidae,

Antilopini, Cephalophinae, etc.) amplitudes of SB in the lumbar and lumbosacral joints are at the level of various carnivores, so these species can be considered "dorsomobile runners" rightfully. Only the larger artiodactyls are characterized by significantly reduced amplitudes of SB in the lumbosacral part of the vertebral column, so these species can be considered "dorsostable runners".

Horses are well-known as dorsostable runners (Hildebrand, 1959). This makes horse riding comfortable. Gambaryan (1974) refers the equid gallop to the cursorial running form. The equid gallop is characterized by a decrease in vertical fluctuations of the center of gravity (no more than 6% of the height at the withers at a galloping speed of 45 km/h in ponies), a reduction of uROM in the limb joints, and an increase in stride frequency (Gambaryan, 1974). The cumulative SB aROM in the lumbosacral part of the backbone of equids (mean = 50.4°) is on average 10° greater than in Giraffidae and Hippopotamidae, and is similar to that of bovines, being on average 10° less than in large antelopes (Belyaev et al., 2021b; Figure 9). Thus, equids are very similar to mediportal-running bovines and some cursorial artiodactyl runners, such as reindeer and wildebeest, in terms of backbone mobility in the sagittal plane.

An example of a different specialization to "dorsostable" running is the tapir gallop. The tapir gallop is characterized by being relatively high in both vertical fluctuations of the center of gravity (more than 14% of the height at the withers at a galloping speed of 35 km/h in *T. terrestris*) and the uROM of the limb joints (Gambaryan, 1974). Structurally, these animals are characterized by a dorsally arched lumbosacral part of the backbone. A similar arching in even-toed ungulates is characteristic of mouse-deer, many small antelopes, roe deer, etc., which have very high SB aROM in the lumbosacral part of the backbone (75-90°; note that these artiodactyls have a few additional SB-capable RfL joints in the posterior thoracic region). In contrast to that, despite the similar arching, the mobility in the lumbosacral part of the backbone of tapirs is half that of these small artiodactyls (~40°). Available recordings and images (Gambaryan, 1974) of galloping tapirs support this conclusion: The rough estimate of cumulative lumbar plus lumbosacral SB uROM during slow rotary gallop in *T. indicus* is ~29°, and during fast rotary gallop in *T. terrestris* is ~34° (Figure 11). Both values closely approach the calculated cumulative SB aROM (~40°) of this part of the backbone and are three times lower than the lumbar+lumbosacral SB uROM of the iconic dorsomobile gallop in greyhounds (Alexander et al., 1985; Muybridge, 1887). As expected, during the fast gallop, the difference between uROM and aROM is smaller than during the slow gallop (~6° vs. ~11°). Gambaryan (1974) refer the tapir gallop to battering-ram running form.

"Dorsostability" is most pronounced in rhinoceroses. Modern-day rhinoceroses are the largest habitually galloping animals. Gambaryan (1974) refer rhinoceroses to the mediportal running form. The cumulative lumbar SB aROM in Rhinocerotidae is the lowest (mean = 29.6°) across all studied odd-toed and even-toed ungulates. The white rhinoceros has an unusual orientation of the spinous processes of the posterior presacral vertebrae. In other extant rhinoceroses, the spinous processes keep posterior inclination throughout the thoracolumbar part of the vertebral column and up to the sacrum (Figure 5g; https://doi.org/10.6084/m9.figshare.21276723). In contrast, in *Ceratotherium simum*, 16th thoracic vertebra has a vertical spinous process, and the last two thoracic vertebra (T17 and T18) and the first two (of three) lumbar vertebrae have a reversed, anterior inclination of the spinous processes (Figure 5c). The opposite inclination of the processes is known as 'anticliny', and the transitional point (here it is T16), as the 'anticlination point'. Counterintuitively, the opposite inclination of the spinous processes has no correlation with the values of SB aROM: the lumbosacral part of the backbone of the *Ceratotherium simum* has the same cumulative sagittal mobility as that of other rhinoceroses. The spinous processes' anticliny in the white rhinoceros is most probably associated with force distribution. The forward inclination of the spinous processes of the posterior presacral vertebrae makes distances between their apices shorter. Therefore, the interspinous ligaments are shorter too and, hence, are more efficient in restricting ventral flexion of the posterior part of the backbone. This increases stiffness of this part in the stages of gallop when only the hindlimbs are on the ground and the spine acts as a cantilever for the forequarters and the head. It can be hypothesized, that the anticlination of the spinous processes in the white rhinoceros is associated with a different mass distribution along the trunk, probably with heavier forequarters and the head than in its relatives.

Our results indicate that perissodactyls show a similarity with artiodactyls in that cursorial runners have the larger and mediportal runners have the smaller cumulative lumbar SB aROM, and battering-ram runners are in-between. However, perissodactyls have significantly lower cumulative SB aROM in the lumbosacral

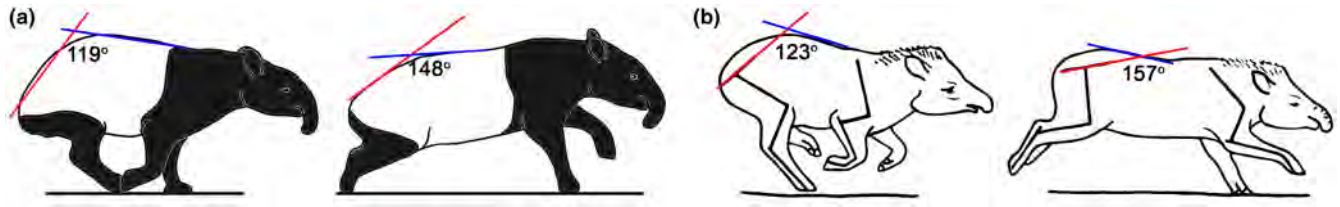

FIGURE 11 Maximum and minimum sagittal curvature of the lumbosacral part of the backbone during (a) slow rotary gallop in *Tapirus indicus* (from https://www.youtube.com/watch?v=UX70MCvtmu0) and (b) fast rotary gallop in *Tapirus terrestris* (modified from Gambaryan, 1974). The difference between the maximum and minimum angles of the curvature represents SB uROM; it equals 29° in (a) and 34° in (b).

part of the backbone than artiodactyls employing the same running forms. Thus, all extant perissodactyls have restricted available sagittal mobility (SB aROM) of the lumbosacral part of the backbone to be used during gallop and can be considered more "dorsostable runners" than artiodactyls in terms of Gambaryan (1974). Among artiodactyls, similar values of SB aROM are found in heavier representatives (Belyaev et al., 2022). Not surprisingly, the mobility of the lumbosacral part of the backbone of the largest galloping mammals, rhinoceroses, is lower than that of any artiodactyl.

As was previously shown for artiodactyls (Belyaev et al., 2021b), the increase in SB aROM (both cumulative and mean) in the lumbar region of the vertebral column is accompanied by elongation of the lumbar region relative to the thoracolumbar part of the backbone as a whole. Vice versa, the decrease in SB aROM is accompanied by relative shortening of the lumbar region. Perissodactyls, with their low lumbar SB aROMs, noted above, also follow this rule. The relative length of lumbar region in Equidae and Tapiridae is similar to that of Giraffidae and Hippopotamidae, which represent the minimum among artiodactyls, and in Rhinocerotidae the lumbar region is even shorter (mean = 14.1% of thoracolumbar length).

Therefore, equids can be regarded as the least dorsostable of extant perissodactyls. If all ungulates were ordered by this trait from the most SB-mobile to the most SB-stable lumbar region, the smaller artiodactyls would be followed by the larger ones together with equids, and the most dorsostable forms would be tapirs and rhinoceroses (Figure 12).

All these findings lead us to the question: why is the lumbosacral part of the backbone in perissodactyls so stiff in the sagittal plane? Is it an ancestral or derived state for representatives of the order? The majority of plesiomorphic Paleogene perissodactyls were very small animals: for example, the equoid *Arenahippus* was around 60–70 cm long and weighed around 9 kg, the tapiroid *Heptodon* weighed around 15 kg, and the rhinocerotoid *Hyrachyus* weighed around 20–50 kg (Radinsky, 1978; Wood et al., 2011). Jones (2016), based on intervertebral joint morphology, stated that increase in body size in equoids correlates with taller, more cordiform vertebral bodies and more dorsally placed zygapophyses, which leads to a reduced sagittal range of motion. We believe that this conclusion is most likely correct because an increase in the relative height of the vertebral body and neural arch pedicles leads to an increase in the radius of sagittal motion (R_{vert}) in the joint, and the R_{vert} increase leads to a decrease in the SB aROM (Belyaev et al., 2022a; Niemeyer et al., 2012). Based on measurements from Wood et al. (2011) the relative length of the lumbar region in *A. grangeri* is 36.8% of thoracolumbar length. This is, on average, 10% longer than in extant equids and is very close to an average for artiodactyls (Belyaev et al., 2021b). Thus, the large number of RfL joints (10) and lumbar vertebrae (7), the absence of intertransverse joints (Wood et al., 2011), the longer lumbar region compared to modern-day equids, and the somewhat lower vertebral bodies and less elevated zygapophysial joints allow us to assume that the lumbar region in small Paleogene equoids was more flexible in the sagittal plane than in extant perissodactyls. The same

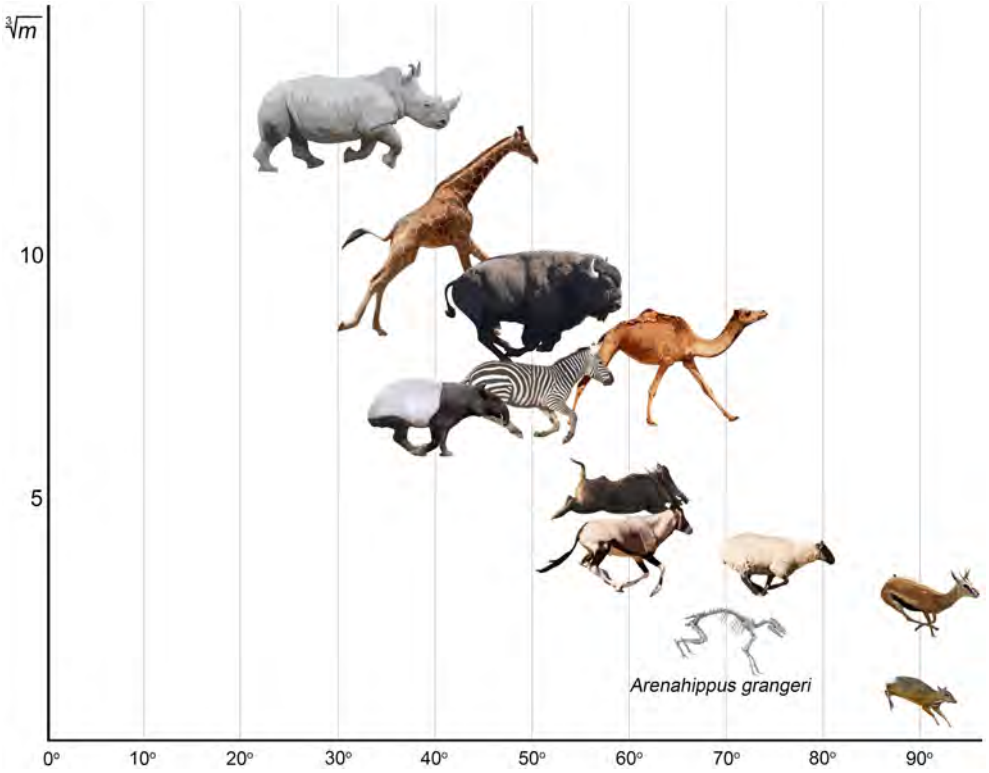

FIGURE 12 Interrelation between sagittal mobility in the lumbosacral part of the backbone and the cube root of body mass in certain typical representatives of odd-toed and even-toed ungulates. *Arenahippus grangeri* (UM 115547) skeleton modified from Wood et al. (2011) and https://umorf.ummp.lsa.umich.edu/wp/specimen-data/?Model_ID=1675. Body masses were taken from Wilson and Mittermeier (2011).

assumption was previously made by Preuschoft and Franzen (2012) and Jones (2016). A longer lumbar region compared to extant species was characteristic of lightly built Paleogene representatives of Ceratomorpha as well. For example, the plesiomorphic Eocene rhinocerotoid *Hyrachyus eximius* was characterized by seven lumbar vertebrae (Cope, 1873; Hayden, 1883). Based on measurements from Cope (1873) the relative length of lumbar region in *H. eximius* (41.5%) is higher than in *A. grangeri* (36.8%), and almost three times exceeds that of extant rhinoceroses (14.1%).

We used 3D models of vertebrae of the *A. grangeri* (UMMP VP 115547) to quantify mobility in the lumbosacral part of the backbone in basal perissodactyls: the low-resolution model from the UMORF website for the T17 and the hi-resolution models for L1 (https://doi.org/10.7302/rh9g-7359) and L2–S1 (https://doi.org/10.7302/81eq-6x84). As a result, we obtained rough SB aROM estimates for four of seven lumbar joints (T17–L4): 7.4° in T17–L1, 7.0° in L1–L2, 9.0° in L2–L3, 8.2° in L3–L4. Extrapolating the mean of these values to all lumbar plus the lumbosacral joint, the cumulative lumbosacral (T17–S1) SB aROM in *A. grangeri* is 63.2°. If we reasonably assume that *Arenahippus* had at least 10° extra SB mobility in the lumbosacral joint compared to the intralumbar joints, then the cumulative SB aROM in the lumbosacral part of the vertebral column should have exceeded 70° (Figure 12).

All the above leads us to assume that dorsostability is a derived feature of extant perissodactyls and evolved convergently in all three families. The two main predictors of SB aROM in the lumbosacral part of the backbone in ungulates are body mass and running form (Belyaev et al. 2021b, 2022). As we previously showed for artiodactyls, the most dorsomobile running forms (saltatorial and saltatorial-cursorial) have an upper limit for body mass (200–300 and 200–400 kg, respectively). With body mass growth to the respective limits, ungulates tend to acquire more size-suitable running forms. All extant species of odd-toed ungulates are medium-to-large animals. The increase in body size in all perissodactyl groups during evolution was accompanied by an increase in food demand and food roughness, which led to the changes in tooth-crown height and occlusal morphology (Fortelius et al., 2006; Janis, 1995; Mihlbachler et al., 2011) and to the increased relative size and complexity of the digestive system enhancing fermentation of cellulose. In case of perissodactyls, it was the hindgut fermentation. It is likely that the size-dependent specialization in the hindgut fermentation led to an increase in the number of vertebrae in order to fit the enlarged abdomen. The heavier the abdomen and the longer the trunk became, the greater the lumbar muscles were loaded. Therefore, these muscles had to be either increased in mass or, preferably, restricted in the range of contraction in favor of force. Thus, the range of contraction of the lumbar muscles was restricted through reduction of SB aROM in posterior thoracic and lumbar joints by replacement of RfL with Tf articulations. This resulted in almost complete disappearance of RfL joints in tapirs and rhinoceroses. Thus, dorsostability allowed the perissodactyls to save on the mass of the backbone muscles in favor of the mass of the hindgut part of the digestive system.

6 | CONCLUSION

Vertebral column morphology and mobility in perissodactyls are very different from artiodactyls. Among perissodactyls, Equidae differ significantly from Ceratomorpha (Tapiridae and Rhinocerotidae) and are closer in some functional features of the backbone to artiodactyls.

As in other mammals, the cervical region is the most mobile part of the vertebral column in the sagittal and frontal planes. Intracervical mobility in the frontal plane in perissodactyls is more than twice as high as that in the sagittal plane. The short and robust neck of modern-day rhinos adapted to support a heavy head, which is used in tournament fights, is characterized by stiff intervertebral joints and low cumulative mobility. The relatively long neck of equids is an agile manipulator, less mobile among ungulates only to camels, llamas, and giraffes. Similarly, to the giraffes, Equidae are characterized by a radial neck-like orientation of zygapophysial articular facets in the T1–T2 joint with a substantially increased SB aROM, which is only slightly lower than that of the cervical joints and is several times higher than that of subsequent thoracic joints.

The thoracolumbar part of the vertebral column in odd-toed ungulates is very stiff in SB. Perissodactyls show frequent vertebral fusions with complete loss of mobility. The thoracic region of perissodactyls includes, on average, five more vertebrae than that of artiodactyls. The anatomy of Paleogene perissodactyls indicates that a large number of thoracic vertebrae is the ancestral state for the order. The number of lumbar vertebrae is significantly decreased in Rhinocerotidae and Tapiridae in favor of the number of thoracic vertebrae. Mean SB aROM values in the posterior half of the thoracic region in Equidae and Rhinocerotidae are the lowest among all studied odd-toed and even-toed ungulates. Thus, the posterior half of the thoracic region in perissodactyls is adapted for dorsostable gallop. This is probably associated with hindgut fermentation in perissodactyls: the increased number of thoracic vertebrae provides additional space for enlarged hindgut, and the sagittal stiffness of posterior thoracic region and reduction of the lumbar region help passively support the hindgut heavily loaded with roughage. This is ensured by an almost complete disappearance of SB-compliant RfL joints in the thoracolumbar part of the backbone of rhinos and tapirs in favor of SB-stiff Tf joints.

The lumbar region in perissodactyls is very stiff in the sagittal plane and is significantly less involved as an active link during gallop than in artiodactyls. The relative length of the lumbar region in Equidae and Tapiridae is similar to the shortest in artiodactyls, and in Rhinocerotidae, it is the shortest among all studied ungulates. The mean SB mobility in the lumbar joints in all three families is at the minimum level for all ungulates. The cumulative lumbosacral SB aROM values in Tapiridae and Equidae are similar to those of the largest artiodactyls, and in Rhinocerotidae they are the lowest across all ungulates. Thus, the lumbar region in all odd-toed ungulates is stiffened in the sagittal plane, along with the posterior thoracic region, and their running can be considered highly "dorsostable" in terms of Gambaryan (1974). Furthermore, rhinoceroses

being the largest habitually galloping mammals are characterized by the most dorsostable condition. The lightly built Eocene ancestors of rhinoceroses and equids were characterized by a longer lumbar region with a larger number of lumbar vertebrae and a higher cumulative SB aROM. All these features together indicate that dorsostability is a derived state of perissodactyls and evolved convergently in the three extant families.

AUTHOR CONTRIBUTIONS

Ruslan I. Belyaev and Natalya E. Prilepskaya worked with material and analyzed the data. All authors wrote the paper, read, and approved the final version of the manuscript.

ACKNOWLEDGMENTS

The authors are very grateful to Alexander Yu. Baranov for his invaluable help in excavating the skeleton of the white rhinoceros. The authors are thankful to the staff of the Rostov-on-Don Zoo and Alexander D. Lipkovich for their hospitality. The authors deeply appreciate and thank Andrey A. Lissovsky (ZMMU), Alexander Bibl (NMW), Gennady F. Baryshnikov, Ekaterina A. Petrova, Mikhail V. Sablin (ZIN) for access to osteological collections; Adam N. Rountrey and Aaron R. Wood for access to 3D models and CT scans of *Arenahippus* vertebrae; Nadezhda V. Kryukova for her help with processing CT scans; Lidiya I. Belyaeva and Yuri V. Belyaev for their overall support; Sergey Sukhovey for his advice and technical support in translation; finally, we also acknowledge two anonymous reviewers and Editor-in-Chief Philip Cox for the valuable advice, which considerably helped improve this research. The study was supported by the Russian Science Foundation (grant no. 22-24-00885).

CONFLICT OF INTEREST

None.

DATA AVAILABILITY STATEMENT

15 figures with photographs of the vertebral column of the studied perissodactyls. All figures: cervical region (C1–T1) left lateral (A) and dorsal (B) view; thoracolumbar and sacral region left lateral (C) and dorsal (D) view (Belyaev et al., 2022b).

ORCID

Ruslan I. Belyaev https://orcid.org/0000-0002-0499-1898
Alexander N. Kuznetsov https://orcid.org/0000-0002-9928-6955
Natalya E. Prilepskaya https://orcid.org/0000-0003-2144-9010

REFERENCES

Alexander, R.M., Dimery, N.J. & Ker, R.F. (1985) Elastic structures in the back and their role in galloping in some mammals. *Journal of Zoology (London)*, 207, 467–482.

Alexander, R.M. & Pond, C.M. (1992) Locomotion and bone strength of the white rhinoceros, *Ceratotherium simum*. *Journal of Zoology*, 227, 63–69. Available from: https://doi.org/10.1111/j.1469-7998.1992.tb04344.x

Audigié, F., Pourcelot, P., Degueurce, C., Denoix, J.M. & Geiger, D. (1999) Kinematics of the equine back: flexion-extension movements in sound trotting horses. *Equine Veterinary Journal. Supplement*, 30, 210–213. Available from: https://doi.org/10.1111/j.2042-3306.1999.tb05219.x

Belyaev, R., Kuznetsov, A. & Prilepskaya, N. (2022b) Figures of various perissodactyls vertebral column. *Figshare*. Figures. Available from: https://doi.org/10.6084/m9.figshare.21276723

Belyaev, R.I. (2018) Vertical intervertebral mobility in representatives of the odd-toed ungulates (Perissodactyla). *Materialy Mezhdunarodnogo molodezhnogo nauchnogo foruma «Lomonosov-2018»*, 1–2. [In Russian].

Belyaev, R.I., Kuznetsov, A.N. & Prilepskaya, N.E. (2021a) A mechanistic approach for the calculation of intervertebral mobility in mammals based on vertebrae osteometry. *Journal of Anatomy*, 238, 113–130. Available from: https://doi.org/10.1111/JOA.13300

Belyaev, R.I., Kuznetsov, A.N. & Prilepskaya, N.E. (2021b) How the even-toed ungulate vertebral column works: comparison of intervertebral mobility in 33 genera. *Journal of Anatomy*, 239, 1370–1399. Available from: https://doi.org/10.1111/JOA.13521

Belyaev, R.I., Kuznetsov, A.N. & Prilepskaya, N.E. (2022a) From dorsomobility to dorsostability: a study of lumbosacral joint range of motion in artiodactyls. *Journal of Anatomy*, 241, 420–436. Available from: https://doi.org/10.1111/joa.13688

Benninger, M.I., Seiler, G.S., Robinson, L.E., Ferguson, S.J., Bonél, H.M., Busato, A.R. & Lang, J. (2004) Three-dimensional motion pattern of the caudal lumbar and lumbosacral portions of the vertebral column of dogs. *American Journal of Veterinary Research*, 65(5), 544–551. Available from: https://doi.org/10.2460/ajvr.2004.65.544

Busscher, I., van der Veen, A.J., van Dieën, J.H., Kingma, I., Verkerke, G.J. & Veldhuizen, A.G. (2010) *In vitro* biomechanical characteristics of the spine: a comparison between human and porcine spinal segments. *Spine*, 35(2), 35–42. Available from: https://doi.org/10.1097/brs.0b013e3181b21885

Canington, S.L., Sylvester, A.D., Burgess, M.L., Junno, J.-A. & Ruff, C.B. (2018) Long bone diaphyseal shape follows different ontogenetic trajectories in captive and wild gorillas. *American Journal of Physical Anthropology*, 167, 366–376. Available from: https://doi.org/10.1002/ajpa.23636

Clayton, H.M. & Townsend, H.G.G. (1989a) Kinematics of the cervical spine of the adult horse. *Equine Veterinary Journal*, 21(3), 189–192.

Clayton, H.M. & Townsend, H.G.G. (1989b) Cervical spinal kinematics: a comparison between foals and adult horses. *Equine Veterinary Journal*, 21(3), 193–195.

Cope, E.D. (1873) On the osteology of the extinct tapiroid *Hyrachyus*. *Proceedings of the American Philosophical Society*, 13(90), 212–224.

Coughlin, B.L. & Fish, F.E. (2009) Hippopotamus underwater locomotion: reduced-gravity movements for a massive mammal. *Journal of Mammalogy*, 90(3), 675–679. Available from: https://doi.org/10.1644/08-MAMM-A-279R.1

Faber, M., Johnston, C., Schamhardt, H., van Weeren, R., Roepstorff, L. & Barneveld, A. (2001a) Basic three-dimensional kinematics of the vertebral column of horses trotting on a treadmill. *American Journal of Veterinary Research*, 62, 757–764.

Faber, M., Johnston, C., Schamhardt, H., van Weeren, R., Roepstorff, L. & Barneveld, A. (2001b) Three-dimensional kinematics of the equine spine during canter. *Equine Veterinary Journal*, 33, 145–149.

Faber, M., Johnston, C., van Weeren, P.R. & Barneveld, A. (2002) Repeatability of back kinematics in horses during treadmill locomotion. *Equine Veterinary Journal*, 34(3), 235–241. Available from: https://doi.org/10.2746/042516402776186010

Faber, M., Schamhardt, H., van Weeren, R., Johnston, C., Roepstorff, L. & Barneveld, A. (2000) Basic three-dimensional kinematics of the vertebral column of horses walking on a treadmill. *American Journal of Veterinary Research*, 61, 399–406.

Filler, A.G. (2007) *Axial character seriation in mammals: an historical and morphological exploration of the origin, development, use, and current collapse of the homology paradigm*. Boca Raton: BrownWalker Press.

Fortelius, M., Eronen, J., Liu, L., Pushkina, D., Tesakov, A., Vislobokova, I. et al. (2006) Late Miocene and Pliocene large land mammals and climatic changes in Eurasia. *Palaeogeography Palaeoclimatology Palaeoecology*, 238(1–4), 219–227.

Gambaryan, P.P. (1974) *How animals run: anatomical adaptations*. New York: John Wiley.

Gambaryan, P.P. & Ruhkyan, R.G. (1974) Morpho-functional analysis of the muscles of the limbs of elephants. *Proceedings of the Zoological Institute of the USSR Academy of Sciences*, 54, 190–265. [In Russian].

Gellman, K.S. & Bertram, J.E.A. (2002) The equine nuchal ligament 2, passive dynamic energy exchange in locomotion. *Veterinary and Comparative Orthopaedics and Traumatology*, 15, 7–14.

Grood, E.S. & Suntay, W.J. (1983) A joint coordinate system for the clinical description of three-dimensional motions: application to the knee. *Journal of Biomechanical Engineering*, 105(2), 136–144.

Gunji, M. & Endo, H. (2016) Functional cervicothoracic boundary modified by anatomical shifts in the neck of giraffes. *Royal Society Open Science*, 3, 150604. Available from: https://doi.org/10.1098/rsos.150604

Gunji, M., Takai, A. & Endo, H. (2014) Deformations of the cervical and cranial thoracic vertebrae in a bedridden Asian elephant. *Japanese Journal of Zoo and Wildlife Medicine*, 19(3), 79–86. Available from: https://doi.org/10.5686/jjzwm.19.79

Haussler, K.K., Bertram, J.E.A. & Gellman, K. (1999) In vivo segmental kinematics of the thoracolumbar spinal region in horses and effects of chiropractic manipulations. *Proc Am Ass equine Practnrs*, 45, 327–329.

Haussler, K.K., Bertram, J.E.A., Gellman, K. & Hermanson, J.W. (2001) Segmental in vivo vertebral kinematics at the walk, trot and canter: a preliminary study. *Equine Veterinary Journal*, 33, 160–164.

Hayden, F.V. (1883) *Report of the United States Geological Survey of the Territories*, Vol. III. Washington, DC: Geological and Geographical Survey of the Territories (U.S.).

Hildebrand, M. (1959) Motions of the running cheetah and horse. *Journal of Mammalogy*, 40, 481–495.

Holbrook, L.T. (2001) Comparative osteology of early tertiary tapiromorphs (Mammalia, Perissodactyla). *Zoological Journal of the Linnean Society*, 132, 1–54. Available from: https://doi.org/10.1111/j.1096-3642.2001.tb02270.x

Hutchinson, J.R., Famini, D., Lair, R. & Kram, R. (2003) Are fast-moving elephants really running? *Nature*, 422(6931), 493–494.

Iimura, T., Denans, N. & Pourqui'e, O. (2009) Establishment of Hox vertebral identities in the embryonic spine precursors. *Current Topics in Developmental Biology*, 88, 201–234.

Janis, C. (1982) Evolution of horns in ungulates: ecology and paleoecology. *Biological Reviews*, 57(2), 261–318. Available from: https://doi.org/10.1111/j.1469-185x.1982.tb00370.x

Janis, C.M. (1995) Correlation between craniodental morphology and feeding behavior in ungulates: reciprocal illumination between living and fossil taxa. In: Thomason, J.J. (Ed.) *Functional morphology in vertebrate paleontology*. Cambridge: Cambridge University Press, pp. 76–98.

Jones, K.E. (2016) New insights on equid locomotor evolution from the lumbar region of fossil horses. *Proceedings of the Royal Society B*, 283, 20152947. Available from: https://doi.org/10.1098/rspb.2015.2947

Jones, K.E., Gonzalez, S., Angielczyk, K.D. & Pierce, S.E. (2020) Regionalization of the axial skeleton predates functional adaptation in the forerunners of mammals. *Nature Ecology & Evolution*, 4, 470–478.

Kambic, R.E., Biewener, A.A. & Pierce, S.E. (2017) Experimental determination of three-dimensional cervical joint mobility in the avian neck. *Frontiers in Zoology*, 14, 37. Available from: https://doi.org/10.1186/s12983-017-0223-z

Kuznetsov, A.N. & Tereschenko, V.S. (2010) A method for estimation of lateral and vertical mobility of platycoelous vertebrae of tetrapods. *Paleontological Journal*, 44(2), 209–225.

Meredith, R., Janečka, J.E., Gatesy, L., Ryder, O.A., Fisher, C.A., Teeling, E.C. et al. (2011) Revolution and KPg extinction on mammal diversification. *Science*, 334(6055), 521–524. Available from: https://doi.org/10.1126/science.1211028

Mihlbachler, M.C., Rivals, F., Solounias, N. & Semprebon, G.M. (2011) Dietary change and evolution of horses in North America. *Science*, 331(6021), 1178–1181. Available from: https://doi.org/10.1126/science.1196166

Muybridge, E. (1887) *Animal locomotion: an electrophotographic investigation of consecutive phases of animal movements*. Philadelphia: University of Pennsylvania.

Narita, Y. & Kuratani, S. (2005) Evolution of the vertebral formulae in mammals: a perspective on developmental constraints. *Journal of Experimental Zoology Part B: Molecular and Developmental Evolution*, 304(2), 91–106.

Niemeyer, F., Wilke, H.J. & Schmidt, H. (2012) Geometry strongly influences the response of numerical models of the lumbar spine—a probabilistic finite element analysis. *Journal of Biomechanics*, 45(8), 1414–1423.

O'Regan, H.J. & Kitchener, A.C. (2005) The effects of captivity on the morphology of captive, domesticated and feral mammals. *Mammal Review*, 35(3–4), 215–230. Available from: https://doi.org/10.1111/j.1365-2907.2005.00070.x

Panjabi, M.M., Crisco, J.J., Vasavada, A., Oda, T., Cholewicki, J., Nibu, K. et al. (2001) Mechanical properties of the human cervical spine as shown by three-dimensional load–displacement curves. *Spine*, 26(24), 2692–2700. Available from: https://doi.org/10.1097/00007632-200112150-00012

Panjabi, M.M., Oxland, T.R., Yamamoto, I. & Crisco, J.J. (1994) Mechanical behavior of the human lumbar and lumbosacral spine as shown by three-dimensional load-displacement curves. *Journal of Bone and Joint Surgery*, 76(3), 413–424.

Panyutina, A.A., Kuznetsov, A.N. & Korzun, L.P. (2013) Kinematics of chiropteran shoulder girdle in flight. *The Anatomical Record*, 296(3), 382–394.

Pourcelot, P., Audigié, F., Degueurce, C., Denoix, J.M. & Geiger, D. (1998) Kinematics of the equine back: a method to study the thoracolumbar flexion-extension movements at the trot. *Veterinary Research*, 9(6), 519–525.

Preuschoft, H. & Franzen, J.L. (2012) Locomotion and biomechanics in Eocene mammals from Messel. *Palaeobio Palaeoenv*, 92, 459–476. Available from: https://doi.org/10.1007/s12549-012-0103-7

Prothero, D. & Schoch, R. (2002) *Horns, tusks, and flippers. The evolution of hoofed mammals*. Baltimore, MD: Johns Hopkins University Press.

Pylypchuk, O.Y. (1975) Roentgenological study of the mobility of a skeleton of the lumbo-sacral region in certain mammals. *Vestnik Zoologii*, 5, 34–38. [In Russian].

Radinsky, L.B. (1965) Evolution of the tapiroid skeleton from *Heptodon* to *Tapirus*. *Bulletin of the Museum of Comparative Zoology at Harvard College*, 134, 69–106.

Radinsky, L.B. (1978) Evolution of brain size in carnivores and ungulates. *The American Naturalist*, 112(987), 815–831.

Regnault, S., Fahn-Lai, P. & Pierce, S.E. (2021) Validation of an echidna forelimb musculoskeletal model using XROMM and diceCT. *Frontiers in Bioengineering and Biotechnology*, 9. Available from: https://doi.org/10.3389/fbioe.2021.751518

Ruiz-García, M., Castellanos, A., Bernal, L.A., Pinedo-Castro, M., Kaston, F. & Shostell, J.M. (2016) Mitogenomics of the mountain tapir (*Tapirus pinchaque*, Tapiridae, Perissodactyla, Mammalia) in Colombia and Ecuador: Phylogeography and insights into the origin and systematics of the south American tapirs. *Mammalian Biology*, 81, 163–175. Available from: https://doi.org/10.1016/j.mambio.2015.11.001

Sánchez-Villagra, M.R., Narita, Y. & Kuratani, S. (2007) Thoracolumbar vertebral number: the first skeletal synapomorphy for afrotherian mammals. *Systematics and Biodiversity*, 5(1), 1–7.

Scott, W.B., Jepsen, G.L. & Wood, A.E. (1941) The mammalian Fauna of the White River Oligocene: part V. Perissodactyla. *Transactions of the American Philosophical Society, New Series*, 28(5), 747–980.

Simpson, G.C. (1945) The principles of classification and a classification of mammals. *Bulletin of the American Museum of Natural History*, 85, 350.

Slijper, E. (1946) Comparative biologic anatomical investigations on the vertebral column and spinal musculature of mammals. *Tweede Sectie*, 17(5), 1–128.

Sokolov, V.E. (1979) *Systematics of mammals (cetaceans, carnivores, pinnipeds, tubulidentata, proboscideans, hyraxes, sirenians, artiodactyls, tylopoda, perissodactyls)*. Moscow: Vysshaya Shkola. [In Russian].

Spoormakers, T.J., Veraa, S., Graat, E.A., van Weeren, P.R. & Brommer, H. (2021) A comparative study of breed differences in the anatomical configuration of the equine vertebral column. *Journal of Anatomy*, 239, 829–838. Available from: https://doi.org/10.1111/joa.13456

Steiner, C.C. & Ryder, O.A. (2011) Molecular phylogeny and evolution of the Perissodactyla. *Zoological Journal of the Linnean Society*, 163(4), 1289–1303. Available from: https://doi.org/10.1111/j.1096-3642.2011.00752.x

Stolworthy, D.K., Fullwood, R.A., Merrell, T.M., Bridgewater, L.C. & Bowden, A.E. (2015) Biomechanical analysis of the camelid cervical intervertebral disc. *Journal of Orthopaedic Translation*, 3(1), 34–43. Available from: https://doi.org/10.1016/j.jot.2014.12.001

Townsend, H.G. & Leach, D.H. (1984) Relationship between intervertebral joint morphology and mobility in the equine thoracolumbar spine. *Equine Veterinary Journal*, 16(5), 461–465. Available from: https://doi.org/10.1111/j.2042-3306.1984.tb01981.x

Townsend, H.G., Leach, D.H. & Fretz, P.B. (1983) Kinematics of the equine thoracolumbar spine. *Equine Veterinary Journal*, 15(2), 117–122.

Vilstrup, J.T., Seguin-Orlando, A., Stiller, M., Ginolhac, A., Raghavan, M., Nielsen, S.C.A. et al. (2013) Mitochondrial Phylogenomics of modern and ancient equids. *PLoS ONE*, 8(2), e55950. Available from: https://doi.org/10.1371/journal.pone.0055950

Wen, N., Lavaste, F., Santin, J.J. & Lassau, J.P. (1993) Three-dimensional biomechanical properties of the human cervical spine in vitro. *European Spine Journal*, 2(1), 2–11.

Wennerstrand, J., Gomez Alvarez, C.B., Meulenbelt, R., Johnston, C., Van Weeren, P.R., Roethlisberger-Holm, K. et al. (2009) Spinal kinematics in horses with induced back pain. *Veterinary and Comparative Orthopaedics and Traumatology*, 22, 448–454.

Werneburg, I., Hinz, J.K., Gumpenberger, M., Volpato, V., Natchev, N. & Joyce, W.G. (2015) Modeling neck mobility in fossil turtles. *Journal of Experimental Zoology Part B: Molecular and Developmental Evolution*, 324(3), 230–243. Available from: https://doi.org/10.1002/jez.b.22557

White, A.A. & Panjabi, M.M. (1990) *Clinical biomechanics of the spine*, 2nd edition. Philadelphia: JB Lippincott.

Wilke, H.J., Geppert, J. & Kienle, A. (2011) Biomechanical in vitro evaluation of the complete porcine spine in comparison with data of the human spine. *European Spine Journal*, 20, 1859–1868.

Wilke, H.J., Herkommer, A., Werner, K. & Liebsch, C. (2017) *In vitro* analysis of the segmental flexibility of the thoracic spine. *PLoS ONE*, 12(5), e0177823. Available from: https://doi.org/10.1371/journal.pone.0177823

Wilke, H.J., Kettler, A. & Claes, L.E. (1997) Are sheep spines a valid biomechanical model for human spines? *Spine*, 22, 2365–2374.

Wilke, H.J., Krischak, S.T., Wenger, K.H. & Claes, L.E. (1997) Load-displacement properties of the thoracolumbar calf spine: experimental results and comparison to known human data. *European Spine Journal*, 6, 129–137.

Wilson, D.E. & Mittermeier, R.A. (2011) *Handbook of the mammals of the world – Volume 2: Hoofed Mammals*. Barcelona: Lynx Ediciones.

Wood, A.R., Bebej, R.M., Manz, C.L., Begun, D.L. & Gingerich, P.D. (2011) Postcranial functional morphology of *hyracotherium* (Equidae, Perissodactyla) and locomotion in the earliest horses. *Journal of Mammalian Evolution*, 18, 1–32. Available from: https://doi.org/10.1007/s10914-010-9145-7

Wu, G., Siegler, S., Allard, P., Kirtley, C., Leardini, A., Rosenbaum, D. et al. (2002) ISB recommendation on definitions of joint coordinate system of various joints for the reporting of human joint motion—part I: ankle, hip, and spine. *Journal of Biomechanics*, 35(4), 543–548.

Wu, G., Van der Helm, F.C., Veeger, H.D., Makhsous, M., Van Roy, P., Anglin, C. et al. (2005) ISB recommendation on definitions of joint coordinate systems of various joints for the reporting of human joint motion—part II: shoulder, elbow, wrist and hand. *Journal of Biomechanics*, 38(5), 981–992.

Yamamoto, I., Kaneda, K. & Panjabi, M.M. (1992) Three-dimensional kinematic analysis of the human whole lumbar spine and natural lumbosacral spondylolysis. In: Niwa, S., Perren, S.M. & Hattori, T. (Eds.) *Biomechanics in orthopedics*. Tokyo: Springer-Verlag, pp. 194–203.

Zarnik, B. (1926) On the ethology of plesiosaurs with contributions to the mechanism of the cervical vertebrae of recent sauropsids. *Societas Scientiarum Naturalium Croatica, Hrvatsko Prirodoslovno Društvo*, 37–38, 424–479. [In Croatian].

SUPPORTING INFORMATION

Additional supporting information can be found online in the Supporting Information section at the end of this article.

How to cite this article: Belyaev, R.I., Kuznetsov, A.N. & Prilepskaya, N.E. (2023) Truly dorsostable runners: Vertebral mobility in rhinoceroses, tapirs, and horses. *Journal of Anatomy*, 242, 568–591. Available from: https://doi.org/10.1111/joa.13799